Intelligent and Converged Networks ISSN 2708-6240
2023, 4(3): 237−260 DOI: 10.23919/ICN.2023.0019

Performance evaluation of DHRR-RIS based HP design using machine learning algorithms

Girish Kumar N G* and Sree Ranga Raju M N

Abstract: Reconfigurable Intelligent Surfaces (RIS) have emerged as a promising technology for improving the reliability of massive MIMO communication networks. However, conventional RIS suffer from poor Spectral Efficiency (SE) and high energy consumption, leading to complex Hybrid Precoding (HP) designs. To address these issues, we propose a new low-complexity HP model, named Dynamic Hybrid Relay Reflecting RIS based Hybrid Precoding (DHRR-RIS-HP). Our approach combines active and passive elements to cancel out the downsides of both conventional designs. We first design a DHRR-RIS and optimize the pilot and Channel State Information (CSI) estimation using an adaptive threshold method and Adaptive Back Propagation Neural Network (ABPNN) algorithm, respectively, to reduce the Bit Error Rate (BER) and energy consumption. To optimize the data stream, we cluster them into private and public streams using Enhanced Fuzzy C-Means (EFCM) algorithm, and schedule them based on priority and emergency level. To maximize the sum rate and SE, we perform digital precoder optimization at the Base Station (BS) side using Deep Deterministic Policy Gradient (DDPG) algorithm and analog precoder optimization at the DHRR-RIS using Fire Hawk Optimization (FHO) algorithm. We implement our proposed work using MATLAB R2020a and compare it with existing works using several validation metrics. Our results show that our proposed work outperforms existing works in terms of SE, Weighted Sum Rate (WSR), and BER.

Key words: Reconfigurable Intelligent Surfaces (RIS); Dynamic Hybrid Relay Reflecting (DHRR)-RIS; Multi User Multiple Input Multiple Output (MU-MIMO); hybrid precoder; machine learning and deep learning algorithms; channel state estimation

1 Introduction

In recent times, the application of Multiple Input Multiple Output (MIMO) antenna technologies has significantly impacted mobile communications, leading to an increase in spectrum efficiency rate[1]. However, a major disadvantage of this adoption is the increased energy consumption. The fully digital beamforming technique, consisting of a digital precoder, was introduced earlier, but the conventional digital precoder had excessive Radio Frequency (RF) chains and high-resolution Digital-to-Analog Converters (DACs), which resulted in increased hardware costs[2, 3]. Similarly, the analog precoder had a similar drawback, but it used high-resolution Analog-to-Digital Converters (ADCs)[4]. To address these issues, researchers have focused on HP and combiner designs that combine digital and analog precoding for MIMO systems, improving beamforming efficiency and reducing hardware losses[5, 6]. Channel State Information (CSI) is a crucial parameter for designing a robust HP/combiner[7]. However, many of the existing works estimate CSI using conventional metrics such as Angle of Arrival (AoA) and Direction of Arrival (DoA) and perform CSI on either the

• Girish Kumar N G is with the Department of Electronics and Telecommunication Engineering, Bangalore Institute of Technology, Visvesvaraya Technological University, Bangalore 560004, India. E-mail: girishkumarng@bit-bangalore.edu.in.
• Sree Ranga Raju M N is with the Department of Electronics and Communication Engineering, Bangalore Institute of Technology, Visvesvaraya Technological University, Bangalore 560004, India. E-mail: mnsrr@rediffmail.com.
∗ To whom correspondence should be addressed.
Manuscript received: 2023-03-05; revised: 2023-05-05; accepted: 2023-06-15

transmitter or receiver side, leading to high computation complexity and channel estimation errors[8, 9].

Reconfigurable Intelligent Surface (RIS) has recently gained attention for mobile network applications, particularly for MIMO-based HP designs and resource allocation[10, 11]. RIS comprises a reflecting element array composed of phase shifters that can passively alter the electromagnetic wave phase, and the reflected signals can be adjusted to the desired direction[12, 13]. Many existing works perform hybrid precoding and combining in passive RIS, making the network highly energy-efficient[14, 15]. However, passive RIS has a major drawback of being fixed in nature and having computation overhead for the transmitter and receiver side[16, 17]. To address this issue, some works incorporate active elements in RIS, consisting of baseband processing units that can perform channel state estimation separately for transmitters and receivers more accurately[18, 19]. Hybrid Relay Reflecting RIS (HRR-RIS) is a combination of passive and active elements expected to be the best option for hybrid precoding design. Recent research adopts machine learning and deep learning algorithms with RIS for designing HP/combiners[20], yet a robust and low-complexity design, in terms of low resolution DAC/ADC, RF chain limitation, and optimal phase shift optimization, has not been precisely optimized.

In this work, we adopt Dynamic Hybrid Relay Reflecting (DHRR)-RIS as shown in Fig. 1 with an artificial intelligence algorithm for designing robust HP/combiners for MIMO that will address all the existing issues.

1.1 Motivation & objective

In recent years, designing optimal HPs and combiners for massive MIMO have posed several challenges. While existing works have made progress in overcoming these challenges, a precise solution has not yet been achieved. Some specific and common issues faced by existing works include high energy consumption, poor Spectral Efficiency (SE), and increased channel estimation errors.

High energy consumption. Majority of existing works design HPs and combiners for massive MIMO by optimizing RF chains and phase shifters in conventional phased array analog beamformers. Phased array analog beamformer is highly energy-consuming when the number of antennas is increased, which attenuates signals and leads to high energy consumption. Even though some works adopt RIS for HPs and combiner designs in MIMO, the elements in

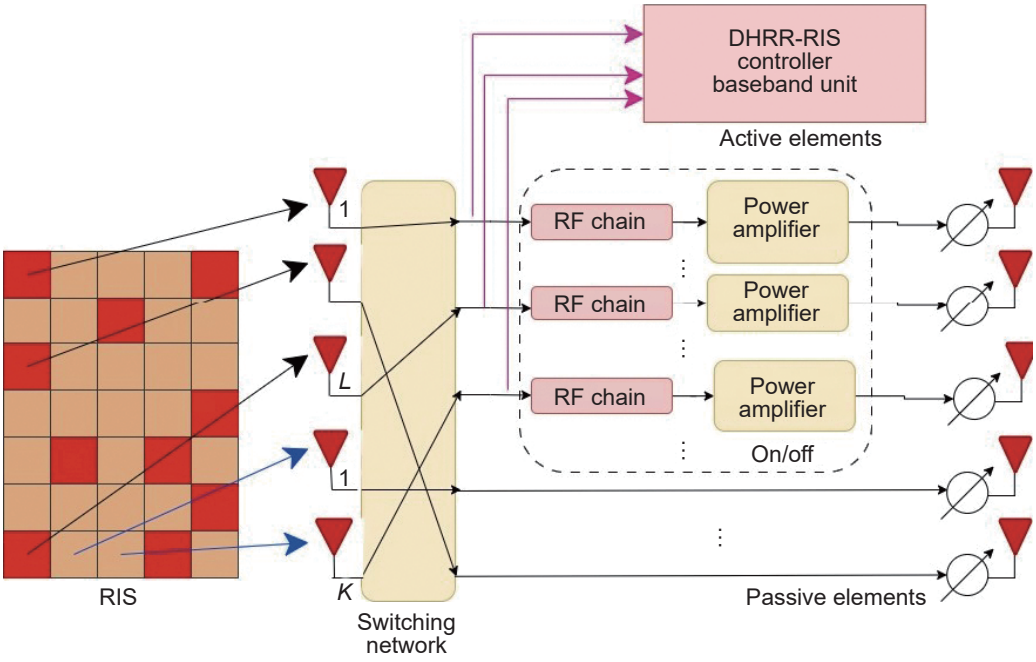

Fig. 1 Design of DHRR-RIS.

the RIS are fixed without considering the dynamicity of the environment, which also leads to high energy consumption.

Poor SE. Most of the existing works have not adequately addressed the optimization of the data stream of the transmitter in designing HPs and combiners for massive MIMO. As the data streams transmitted by the transmitter are massive, optimizing the data stream is necessary to enhance the SE of the framework. However, most of the state-of-the-art works have not fully leveraged data stream optimization, and this has negatively impacted the SE of the framework.

Increased channel estimation errors. The existing works for channel estimation in massive MIMO systems considers only limited metrics such as AoA and DoA, leading to increased channel estimation errors. Moreover, most of these works performs channel estimation at the transmitter or receiver, which increases hardware complexity and computation overhead, leading to further channel estimation errors.

Based on the challenges mentioned, the proposed work aims to address the issue by designing an energy-efficient, low-complexity HP for massive MIMO systems. The research objective is to use deep learning methods to design a low-complexity HP with low-resolution ADC/DAC for massive MIMO systems. This research also aims to address the issues related to channel estimation and SE in existing works.

Some of the sub-objectives of this research are:

• To reduce channel estimation errors and computation overhead by constraining pilot signals and performing channel estimation on the DHRR-RIS side using a machine learning algorithm.

• To enhance SE and reduce complexity by optimizing the data stream into clusters and scheduling them into two-time scales.

• To mitigate power and phase errors by adopting one-bit DAC/ADC and vector modulated phase shifters for massive MIMO.

• To ensure a robust HP design by performing joint optimization of RF-DAC/ADC pairs in the transmitter/receiver side and phase shifter in the DHRR-RIS side, respectively.

1.2 Research contributions

The proposed research focuses on the development of a low-complexity HP for massive MIMO systems using AI algorithms and DHRR-RIS. The key contributions are listed as follows:

• Designing a dynamically adjustable DHRR-RIS architecture that enhances scalability and adaptability in Multi User MIMO (MU-MIMO) systems, offering a more flexible and adaptable communication system compared to traditional designs.

• Utilizing adaptive threshold-based pilot optimization and Adaptive Back Propagation Neural Network (ABPNN) algorithms for efficient CSI estimation, addressing complexity issues related to increased pilot transmission, high Bit Error Rate (BER), and high channel estimation errors.

• Enhanced Fuzzy C-Means (EFCM) clustering algorithm and two-time scale scheduling for data stream optimization and management, addressing SE issues caused by increased data stream transmission.

• Implementing cooperative hybrid precoding by optimizing the Base Station (BS) digital precoder using Deep Deterministic Policy Gradient (DDPG) and the analog precoder using Fire Hawk Optimization (FHO) in a cooperative manner.

• Evaluating the proposed HP design's efficacy through MATLAB R2020a simulations and comparing it with existing works using metrics such as Weighted Sum Rate (WSR) (bits/Hz), BER, and SE (bps/Hz), demonstrating the advantages of incorporating RIS technology into massive MIMO systems.

2 Paper organization

The remaining of the paper is organized as follows: Section 3 provides the literature survey and corresponding gaps of the state-of-the-art works. Section 4 emphasizes the system model in which the channel model and problem formulation are analysed. Section 5 explains the proposed methodology with proper explanation and suitable pseudocode and diagrams. Section 6 provides the experimental results with simulation setup, comparative analysis, complexity analysis, and research summary. Section 7 concludes the proposed research. The notations used in

this research are listed in Table 1.

3 Literature survey

This section aims to provide a comprehensive review of the current research on HP design, with a focus on the gaps in the literature. To aid in comprehension, this section is divided into two subsections: RIS-based HP design and HP design without RIS. Additionally, Table 2 summarizes the gaps in the existing research, along with the simplified algorithms/methods that are used.

3.1 RIS aided channel estimation & HP design using AI and other methods

The rapid development of RIS has led to multiple approaches for enhancing massive MIMO communication networks. We examine key works, highlighting our HP-DHRR-RIS model's merits. Reference [21] adopts a deep learning-based hybrid precoding approach for MIMO-enabled THz communication using RIS but overlooks data stream optimization and scheduling, essential components of our model. Reference [22] presents a dual RIS-assisted multi-user MIMO mmWave system with hybrid precoding but does not address complexities related to pilot and CSI optimization. In contrast, our model employs an adaptive threshold method and an ABPNN for optimizing pilot and CSI. Reference [23] describes a multi-hop RIS-empowered terahertz communication system using deep reinforcement learning for hybrid beamforming design. Although it provides optimized policy for precoder optimization, it does not tackle challenges related to data stream optimization, SE, and energy consumption. Our proposed model overcomes these limitations by classifying data streams using an EFCM algorithm and scheduling them based on priority and emergency levels. Reference [24] applies a distributed machine learning algorithm for downlink channel estimation in RIS-assisted wireless communications but neglects the optimization of digital and analog precoders. In contrast, our model employs an DDPG algorithm for digital precoder optimization and an FHO algorithm for analog precoder optimization.

Authors in Refs. [25–27] outline various methods for RIS-assisted MIMO systems and hybrid precoding. While valuable, they did not explicitly address challenges tackled by our HP-DHRR-RIS model, such as SE, WSR, and BER.

In summary, our proposed HP-DHRR-RIS model surpasses existing research by addressing limitations in current works, offering a more robust solution for RIS-assisted MIMO communication networks. Focusing on low-complexity design, SE, WSR, and BER, and energy consumption, our approach demonstrates significant improvements over existing techniques, contributing to the field's continued progression.

Table 1 List of notations.

Notation	Description
A_{t} & A_{r}	Transmitter & receiver antennas
$J_{\mathrm{t}} \in C^{A\times A_{\mathrm{t}}}$	Channel between BS and DHRR-RIS
$J_{\mathrm{r}} \in C^{A_{\mathrm{r}}\times A}$	Channel between user and DHRR-RIS
$\mathrm{pow}^{\mathrm{BS}}$	Power at the base station
N	Noise at the user
N_{J}, N_{US}	Noise at DHRR-RIS and user, respectively
$\beta_{n,m}^{(q)}$	Path gain
α_k	Relay/reflection co-efficient
R	Covariance matrix
b^{opt}	Beamforming matrix
P	Pilot sequences
$\mathfrak{p}$	Estimated channel vector
$\mathfrak{Q}\left[\widehat{\mathrm{cV}}_{\mathrm{rcon}}\right]$	Quantized channel vector
$\mathfrak{I}(\mathfrak{U},\mathfrak{V})$	Fuzzy objective function
Y	Scheduling constant
F_{AP} and F_{DP}	Analog and digital precoder
CM	Channel matrix
$\mathrm{VM}_{\mathrm{ps}}$	Vector modulated phase shifters
$y\mathfrak{x}_z^{\mathrm{dl}}$ and $y\mathfrak{x}_{z*}^{\mathrm{ul}}$	Pilot sequence of the receivers and transmitters

3.2 RIS unaided chanel estimation & HP design using machine learning and other algorithms

The proposed HP-DHRR-RIS model exhibits significant improvements over current methodologies by incorporating RIS technology, which is often absent in existing works. Contrasted with the two-timescale end-to-end learning in Ref. [28], our model utilizes an adaptive threshold method and ABPNN, providing enhanced pilot signal optimization and CSI acquisition, effectively addressing the limitations of Ref. [28]. In comparison to the deep learning-based joint CSI

Table 2 Analysis of the gaps in the existing research.

Category	Reference	Method utilized	Objective	Pros and Cons
RIS aided channel estimation & HP design using AI and other methods	[21]	Parallel deep neural network and zero forcing algorithm	Hybrid precoding design for THz communication using RIS	• High computational & hardware complexity • High noise amplification in multi user scenario
	[22]	Reimannian joint optimization algorithm	Dual RIS based hybrid precoding design for MU-MIMO	• High channel estimation • Poor SE and high energy consumption • Not be suitable for unstructured data, such as images or audio
	[23]	Deep reinforcement algorithm and joint optimization method	RIS-based hybrid precoding design for THz communication	• Less beamforming efficiency • Increased channel estimation errors
	[24]	Distributed machine learning algorithm	RIS-based estimation of downlink channels in wireless environment	• Increased errors and deprived data interpretation
	[25]	Element wise minimized symbol error rate and vector gradient based minimized symbol error rate	Precoder and reflection design in cooperative manner using RIS for MIMO	• Not suitable for dynamic environments
	[26]	Channel estimation based of decomposition method	Designing of HPs and adjustment of RIS in cooperative manner	• High root mean square and phase errors
	[27]	Joint optimization of ADC and RIS power	Effective beamforming for MIMO using RIS-based ADCs	• High complexity for channel estimation at both the transmitter and receiver side, respectively
RIS unaided channel estimation & HP design using AI and other methods	[28]	Dual time scale and deep neural networks	Hybrid precoding design and channel estimation based on dual time scales	• High energy consumption • Less accurate channel estimations
	[29]	Convolutional neural network & deep neural network	Cooperative design of hybrid precoding and CSI feedback optimization using DL	• High computational overhead • Less energy efficiency
	[30]	Convolutional neural network	Hybrid precoding design for mmWave MIMO using DL	• Less SE • Poor results in RF chain optimization
	[31]	Machine learning algorithm, Dinklebach method, and water filling algorithm	Hybrid precoding design for mmWave MIMO using ML with domestic switch network	• High hardware complexity • Not suitable for dynamic environment
	[32]	Deep neural network and zero forcing algorithm	DL-based channel estimation and hybrid precoding design for mmWave MIMO	• High noise amplification for digital precoder design
	[33]	Deep neural networks	DL-based channel sensing and HP design using mmWave MIMO	• High complexity and computational overhead
	[34]	Convolutional neural network and hierarchical codebook algorithm	DL-based channel estimation & hybrid precoding for mmWave MIMO	• Poor channel state estimation
	[35]	Greedy selection cross validation method	Estimating resilient channel for mmWave MIMO using ADCs	• High squared loss errors
	[36]	Machine learning algorithm	Utilizing low resolution analog PS for HP design using ML	• Not focusing on data stream optimization • Less SE
	[37]	ID convolutional neural network	Adopting DL algorithm of channel estimation of geospatial data for mmWave MIMO	• High problem of overfitting

(To be continued)

Table 2 Analysis of the gaps in the existing research. (Continued)

Category	Reference	Method utilized	Objective	Pros and Cons
RIS unaided channel estimation & HP design using AI and other methods	[38]	Deep neural networks	Realizing the robust precoding by adopting DL-based hybrid precoding	• High errors during channel estimation
	[39]	Precoder networks	DRL-based hybrid beamforming for mmWave MIMO	• High consumption of energy • High signal attenuation
	[40]	Distributed neural precoding and deep neural network	For mmWave MIMO distributed precoding was performed using DL	• Poor results due to lack of learning optimal features
Proposed work (HP-DHRR-RIS)		Adaptive back propagation neural network, enhanced fuzzy c-means, deep deterministic policy gradient, and fire hawk optimization	Designing an energy effective low complexity HP design of MU-MIMO using AI based on DHRR-RIS	• Less channel estimation errors • High SE • Power reduction high energy efficiency

feedback and hybrid precoding in FDD mmWave massive MIMO systems in Ref. [29], our approach employs RIS technology and the EFCM algorithm to enhance beam alignment and system performance, leading to more dynamic resource allocation.

Our model outperforms the deep CNN and equivalent channel-based hybrid precoding in Ref. [30] by optimizing the digital and analog precoders at the BS and DHRR-RIS, respectively, resulting in a more robust and efficient communication system. Differing from the machine learning-inspired hybrid precoding in Ref. [31], our model integrates RIS technology for superior optimization of digital and analog precoders and improved system performance. Our model demonstrates enhanced performance over the sparse channel estimation and hybrid precoding using deep learning in Ref. [32] due to the incorporation of RIS technology, resulting in more accurate channel estimation. By leveraging RIS technology and optimizing the digital and analog precoders at the BS and DHRR-RIS, our model outperforms the deep learning-based channel sensing and hybrid precoding in Time Division Duplexing (TDD) massive MIMO Orthogonal Frequency Division Multiplexing (OFDM) systems in Ref. [33], enabling better interference management. In contrast to the deep learning-based channel estimation and hybrid precoding for millimeter wave communications in Ref. [34], our model employs RIS technology to optimize pilot signals, CSI, and data streams for superior link adaptation.

Our approach exhibits improved performance in terms of SE, WSR, and BER over the spatial wideband channel estimation in Ref. [35] by incorporating RIS technology and optimizing data streams, leading to a more robust and efficient communication system. Our model surpasses the machine learning-based hybrid precoding in Ref. [36] and the deep learning and geospatial data-based channel estimation technique in Ref. [37] by employing RIS technology and optimizing the digital and analog precoders at the BS and DHRR-RIS, resulting in a more advanced and efficient communication system with better channel estimation accuracy. In comparison to the deep learning-based robust precoding for massive MIMO in Ref. [38], our approach addresses limitations by incorporating RIS technology and optimizing digital and analog precoders, leading to a more advanced and efficient system with superior precoding robustness. In contrast to the PrecoderNet hybrid beamforming in Ref. [39], our model integrates RIS technology for improved optimization of digital and analog precoders and better handling of millimeter wave channel characteristics. Lastly, our HP-DHRR-RIS model exhibits significant advantages over the Distributed Neural Precoding (DNP) technique in Ref. [40] by incorporating RIS technology, optimizing the digital and analog precoders at the BS and DHRR-RIS, and reducing overhead in feedback signaling.

In conclusion, our HP-DHRR-RIS model outperforms existing methods in the literature by integrating RIS technology and optimizing digital and analog precoders. This approach achieves enhanced

communication performance through improved channel estimation, beam alignment, and interference management, resulting in a more advanced and efficient communication system.

4 System model

The BS and Users (US) are the primary entities involved in the design of an HP for downlink data transmission. However, in situations where direct links between the BS and US are hindered by blockages or path loss, alternative solutions such as the proposed DHRR-RIS can be introduced to facilitate beamformed communication by designing optimal HPs and combiners between the entities. The antennas situated in the BS and US are denoted as A_{t} and A_{r}, respectively. The channel between the DHRR-RIS and US can be represented as $J_{\mathrm{r}} \in C^{A_{\mathrm{r}} \times A}$, while the channel between the BS and DHRR-RIS can be denoted as $J_{\mathrm{t}} \in C^{A \times A_{\mathrm{t}}}$, where A is the dynamic set of active elements in DHRR-RIS. The transmission signal vector can be represented as $y \in C^{A_{\mathrm{t}} \times 1}$, where $\{yy^{\mathrm{H}}\} = \mathrm{pow}^{\mathrm{BS}} \times I_{A_{\mathrm{r}}}$, with $\mathrm{pow}^{\mathrm{BS}}$ denoting the transmission power. $\Phi = \mathrm{Dia}\{\Phi_1, \Phi_2, \ldots, \Phi_M\}$ and $\Psi = \mathrm{Dia}\{\Psi_1, \Psi_2, \ldots, \Psi_M\}$, where M is total number of active and passive reflecting elements in DHRR-RIS. The received signal at the US can be expressed as follows:

$$x = J_{\mathrm{r}} \Phi J_{\mathrm{t}} y + J_{\mathrm{r}} \Psi J_{\mathrm{t}} y + J_{\mathrm{r}} \Psi N_J + N_{\mathrm{US}} \tag{1}$$

By simplifying Eq. (1)

$$=> (J_{\mathrm{r}} \Psi J_{\mathrm{t}} + J_{\mathrm{r}} \Phi J_{\mathrm{t}}) y + N \tag{2}$$

$$=> J_{\mathrm{r}} \Lambda J_{\mathrm{t}} y + N \tag{3}$$

From Eqs. (2) and (3), the overall noise at the US can be denoted as $N = J_{\mathrm{r}} \Psi N_J + N_{\mathrm{US}}$. The vectors of complexity additive white gaussian noise at the DHRR-RIS and US can be denoted as $N_J \sim \mathcal{CN}(0, \delta_J^2 I_M)$ and $N_{\mathrm{US}} \sim \mathcal{CN}(0, \delta_{\mathrm{US}}^2 I_{A_{\mathrm{r}}})$ respectively in which the M denotes the number of sub-surfaces in the DHRR-RIS. For simplifying the complex notation in the above equations, we have assumed $\delta_{\mathrm{US}}^2 = \delta_J^2 = \delta^2$ in which $N \sim \mathcal{CN}\left(0, \delta^2 \left(I_{A_{\mathrm{r}}} + J_{\mathrm{r}} \Psi \Psi^{\mathrm{H}} J_{\mathrm{r}}^{\mathrm{H}}\right)\right)$.

4.1 Channel model

The proposed methodology employs the Saleh−Valenzuela (S−V) channel model to analyse the targeted environment. The S−V channel model is composed of time-based stochastic properties that are well-suited for analysing wireless environments with multiple propagation paths. Based on the system model design, the channel vector $j_{n,m}$ can be formulated as follows:

$$j_{n,m} = \sqrt{\frac{K}{Q_{n,k}}} \sum_{q=0}^{Q_{n,k}} \beta_{n,m}^{(q)} b\left(\varphi_{n,m}^{(q)}, \theta_{n,m}^{(q)}\right) \tag{4}$$

From the above equation, $j_{n,m}$ represents the channel vectors, $Q_{n,k}$ denotes the number of multipath among the n-th user and m-th sub-surface of the DHRR-RIS, K represents the number of passive elements in the DHRR-RIS. The gain of the q-th path can be denoted as $\beta_{n,m}^{(q)}$. $\varphi_{n,m}^{(q)}$ and $\theta_{n,m}^{(q)}$ are elevation and azimuth Angle of Departure (AoD) of the q-th path respectively $(1 \leqslant q \leqslant Q_{n,k})$ in which the vector array response can be represented as $b\left(\varphi_{n,m}^{(q)}, \theta_{n,m}^{(q)}\right) \in D^{M_m \times 1}$. When we consider the antenna in Uniform Planar Antenna (UPA) array, the elements of an antenna in a vertical manner is M_{m_1} and the elements of an antenna in a horizontal direction is M_{m_2} (i.e., $M_m = M_{m_1} \times M_{m_2}$). The overall array response vector can be formulated as

$$b(\varphi, \theta) = b_{\mathrm{azi}}(\varphi) \otimes b_{\mathrm{ele}}(\theta) \tag{5}$$

where $b_{\mathrm{azi}}(\varphi)$ and $b_{\mathrm{ele}}(\theta)$ can be expanded as

$$b_{\mathrm{azi}}(\varphi) = \frac{1}{\sqrt{M_{m_1}}} \left[\mathrm{e}^{\mathrm{j}2\pi i(\mathrm{di}_1/\lambda)\sin(\varphi)}\right]^{\mathrm{T}}, i \in I\left(M_{m_1}\right) \tag{6}$$

$$b_{\mathrm{ele}}(\theta) = \frac{1}{\sqrt{M_{m_2}}} \left[\mathrm{e}^{\mathrm{j}2\pi i(\mathrm{di}_2/\lambda)\sin(\theta)}\right]^{\mathrm{T}}, i \in I\left(M_{m_2}\right) \tag{7}$$

From the above equations, the wavelength is represented as λ, the element spacing direction in vertical and horizontal can be denoted as di_1 and di_2 respectively in which $I(n) = \{0, 1, \ldots, n-1\}$.

4.2 Problem formulation

The SE and achievable sum rate during the precoding design of the DHRR-RIS based MU-MIMO can be formulated based on Eq. (1) as follows:

$$f_0(\{\alpha_k\}) = \log_2 \left| I_{A_{\mathrm{r}}} + \gamma J_{\mathrm{r}} \Lambda J_{\mathrm{t}} J_{\mathrm{t}}^H \Lambda^H J_{\mathrm{r}}^H R^{-1} \right| \tag{8}$$

In the SE equation mentioned above, the reflecting/relay elements set in the DHRR-RIS is denoted by $\{\alpha_k\} = \{\alpha_1, \alpha_2, \ldots, \alpha_K\}$, and Λ represents a diagonal matrix of the surface. The covariance matrix

of noise in an aggregated manner is denoted by R and can be formulated as follows:

$$R = I_{A_\mathrm{r}} + J_\mathrm{r} \Psi \Psi^H J_\mathrm{r}^H \in C^{A_\mathrm{r} \times A_\mathrm{r}} \tag{9}$$

γ can be denoted as $\gamma = \dfrac{\mathrm{pow}^{\mathrm{BS}}}{\delta^2}$. The power transmission of active/passive elements in the DHRR-RIS can be expressed as

$$\begin{aligned} \mathrm{pow}_{\mathrm{ac/pas}}(\{\alpha_k\}) \triangleq & \mathrm{trace}\left(\Psi\left(J_\mathrm{t} E\left\{yy^\mathrm{H}\right\} J_\mathrm{t}^\mathrm{H} + \delta^2 I_K\right)\Psi^\mathrm{H}\right) = \\ & \mathrm{trace}\left(\Psi\left(\mathrm{pow}^{\mathrm{BSS}} J_\mathrm{t} J_\mathrm{t}^\mathrm{H} + \delta^2 I_K\right)\Psi^\mathrm{H}\right) \end{aligned} \tag{10}$$

The problem formulation of reflection/relay surfaces in the DHRR-RIS for maximizing the SE can be expressed as

$$\begin{gathered} \max_{\{\alpha_k\}} f_0(\{\alpha_k\}), \\ \text{subject to } |\alpha_k| = 1, \text{ for } k \notin A, \\ \mathrm{pow}_{\mathrm{ac}}(\{\alpha_k\}) \leqslant \mathrm{pow}_{\mathrm{ac}}^{\max} \end{gathered} \tag{11}$$

where $f_0(\{\alpha_k\})$ is a non-convex function based on $\{\alpha_k\}$, and the power budget of the active elements in the DHRR-RIS can be denoted as $\mathrm{pow}_{\mathrm{ac}}^{\max}$.

$$\forall = \sum_{k=1}^{K} \log_2(1 + \mathrm{SINR}_k) \tag{12}$$

where SINR_k is the signal io interference plus noise ratio of the k-th user which is formulated as

$$\mathrm{SINR}_k = \frac{\left| {j_k}^\mathrm{H} f_{\mathrm{AP}} \Lambda {f_{\mathrm{DP}}}^k \right|}{\sum_{k' \neq k}^{K} \left| {j_k}^\mathrm{H} f_{\mathrm{AP}} \Lambda {f_{\mathrm{DP}}}^{k'} \right| + \delta^2} \tag{13}$$

The problem of maximizing the achievable sum rate can be formulated as

$$\begin{gathered} \left({F_{\mathrm{AP}}}^{\mathrm{opt}}, {F_{\mathrm{DP}}}^{\mathrm{opt}}\right) = \arg\max_{\mathrm{b,pre}} \forall \\ \text{Subject to } c_1 : \|F_{\mathrm{DP}}\|_{F_{\mathrm{DP}}}^2 \leqslant \mathrm{pow} \\ c_2 : F_{\mathrm{AP}} \in \zeta \end{gathered} \tag{14}$$

where ${F_{\mathrm{AP}}}^{\mathrm{opt}}$ denotes the matrix for beamforming, and ${F_{\mathrm{DP}}}^{\mathrm{opt}}$ denotes the matrix for precoding. The set of analog beamforming matrices is denoted as ζ.

5 HP-DHRR-RIS model

The primary objective of this research is to design low-complexity HPs/combiners for massive MIMO systems using artificial intelligence algorithms. The proposed methodology adopts DHRR-RIS for HP design in MIMO systems to reduce energy consumption and hardware losses, while improving system performance. Additionally, the proposed methodology achieves dynamic adaptation to channel conditions by utilizing DHRR-RIS. Furthermore, the adoption of one-bit DAC/ADC at the transmitter and receiver side reduces power consumption and hardware costs in MIMO systems. The entities involved in the proposed work are receivers (i.e., users), transmitters (i.e., base station), and controllers. The controller is responsible for controlling the DHRR-RIS, which consists of four sub-entities: mapping entity, optimization entity, DRL entity, and RIS entity. The mapping entity is responsible for pilot optimization and CSI estimation, the optimization entity optimizes the transmitter data streams, and the DRL entity and RIS entity design the HP/combiner by utilizing two learning agents. Figure 2 represents the complete architecture of the proposed MU-MIMO based DHRR-RIS for HP design. The processes involved in the proposed methodology are as follows:

- DHRR-RIS design;
- Machine learning based CSI estimation;
- Data stream optimization & scheduling;
- DRL-based cooperative HP design.

5.1 DHRR-RIS design

The proposed work aims to address the limitations of conventional RIS by designing a DHRR-RIS that overcomes issues related to CSI acquisition and phase control. Instead of using phased array analog precoders, the proposed approach employs DFRR-RIS based analog precoding design, or analog beamforming. The DHRR-RIS comprises both passive (K) and active (L) elements, which are collectively represented as $M = K + L$. The passive elements serve as the reflecting elements or analog beamformers, utilizing vector modulated phase shifters to reflect beams in desired directions. The use of vector modulated phase shifters, as opposed to conventional phase shifters, reduces phase errors. The components involved in the vector modulated phase shifters include two hybrid couplers, two single pole double throw switches, four buffer amplifiers, one Marchand balun, and two Variational Gain Amplifiers (VGAs), which

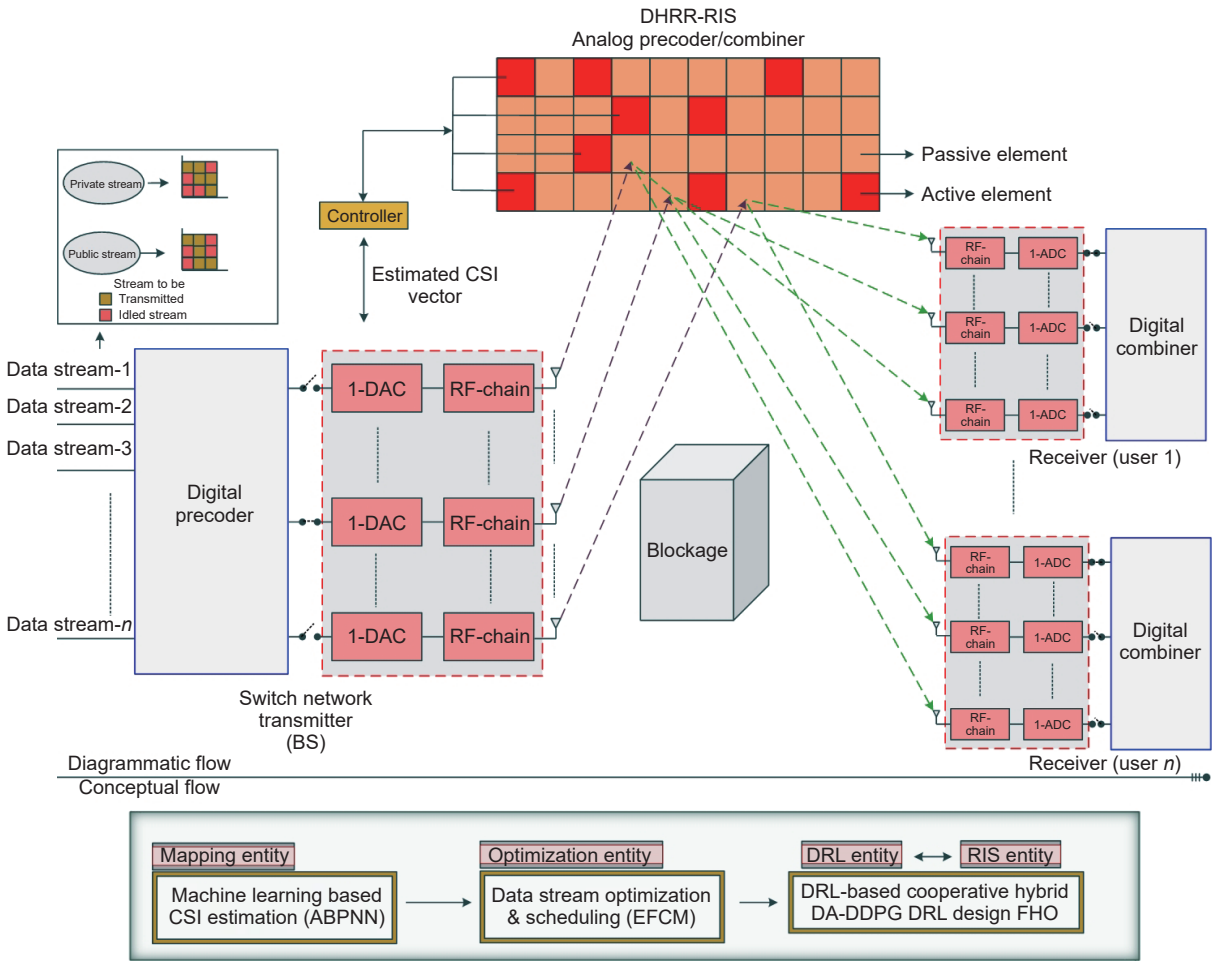

Fig. 2 Overall architecture of proposed HP-DHRR-RIS design.

work together to minimize phase errors and generate wideband differential signals.

The proposed DHRR-RIS includes both passive and active elements. The passive elements act as the analog beamformer and consist of vector modulated phase shifters to reflect the beams in the desired position. Vector modulated phase shifters are adopted to reduce phase errors, and the components involved in the phase shifters include two hybrid couplers, two single pole double throw switches, four buffer amplifiers, one Marchand balun, and two VGAs.

The active elements, on the other hand, are responsible for separately estimating the channel states for the transmitter and receiver. It should be noted that the power consumption of active elements is higher than that of passive elements due to the presence of RF chains and power amplifiers.

The dynamic set of active elements in the proposed DHRR-RIS can be denoted as A, where A is a subset of $\{1, 2,..., M\}$. The reflection/relay coefficient can be formulated as:

$$\alpha_k = \begin{cases} |\alpha_k| e^{j\theta_k}, & \text{if } k \in A; \\ e^{j\theta_k}, & \text{otherwise} \end{cases} \tag{15}$$

From Eq. (15), the phase shift is denoted as $\theta_k \in [0, 2\pi]$. For $k \notin A$, the $|\alpha_k| = 1$. There are three diagonal matrices are defined based on $|\alpha_k|$.

The diagonals are represented as $\Phi = \text{Dia}\{\Phi_1, \Phi_2, \ldots, \Phi_M\}$, $\Lambda = \text{Dia}\{\Lambda_1, \Lambda_2, \ldots, \Lambda_M\}$, and $\Psi = \text{Dia}\{\Psi_1, \Psi_2, \ldots, \Psi_M\}$. Based on the expressed diagonal matrices, the following expression by $|\alpha_k| = 1$ can be derived as

$$\Phi_k = \begin{cases} 0, & \text{if } k \in A; \\ \alpha_k, & \text{otherwise} \end{cases}, \Psi_k = \begin{cases} 0, & \text{if } k \in A; \\ \alpha_k, & \text{otherwise} \end{cases} \tag{16}$$

From Eq. (16), it is inferred that the diagonals Ψ_k and Φ_k are composed only with dynamically adjusted reflecting elements. Λ is composed with all elements of

DHRR-RIS. So that, $\Lambda = \Psi + \Phi$. Further, based on the varying channel condition and data stream flows, the active and passive elements are dynamically on/off by the switch networks. By doing so, the unwanted energy and power consumption in the entities get reduced. Figure 1 represents the detailed model of the proposed DHRR-RIS.

5.2 Machine learning based CSI estimation

The mapping entity in the proposed DHRR-RIS system is responsible for accurately estimating the CSI separately for the BS transmitters and US receivers. While the BS has sufficient power to perform channel estimation, the dynamic nature of the environment may lead to errors in estimation. Therefore, the mapping entity is employed to ensure accurate estimation.

To reduce pilot overhead, the mapping entity constrains the pilot signals sent by both the transmitters and receivers. Specifically, the pilot sequence sent by the receivers is expressed using the equation provided earlier.

$$y\mathfrak{x}_z^{\mathrm{dl}} = \left(\mathrm{FAc}_{\mathrm{R}}^z \mathrm{FAc}_{\mathrm{B}}^z\right)^{\mathrm{T}} \mathrm{CM}^{\mathrm{T}} P + \left(\mathrm{FAc}_{\mathrm{R}}^z \mathrm{FAc}_{\mathrm{B}}^z\right)^{\mathrm{T}} A_z \quad (17)$$

Similarly, the pilot sequence from the transmitter to the mapping entity can be formulated as,

$$y\mathfrak{x}_{z^*}^{\mathrm{ul}} = \left(\mathrm{FAp}_{\mathrm{R}}^{z^*} \mathrm{FAp}_{\mathrm{B}}^{z^*}\right)^{\mathrm{T}} \mathrm{CM}^{\mathrm{T}} P + \left(\mathrm{FAp}_{\mathrm{R}}^{z^*} \mathrm{FAp}_{\mathrm{B}}^{z^*}\right)^{\mathrm{T}} A_{z^*} \quad (18)$$

In Eqs. (17) and (18), $y\mathfrak{x}_z^{\mathrm{dl}}$ and $y\mathfrak{x}_{z^*}^{\mathrm{ul}}$ represent the downlink pilot sequence sent by the US for z times and the uplink pilot sequence sent by the BS for z^* times, respectively. $\mathrm{FAc}_{\mathrm{R}}^z$ and $\mathrm{FAc}_{\mathrm{B}}^z$ denote the analog and digital combining matrices, while $\mathrm{FAp}_{\mathrm{R}}^z$ and $\mathrm{FAp}_{\mathrm{B}}^z$ represent the analog and digital precoding matrices, respectively. The channel matrix is represented by CM and $P \in C^{\mathrm{BS}\times\mathrm{US}}$ denotes the orthogonal pilot sequences sent by the BS and US, respectively. However, continuously transmitting pilot sequences from both entities can result in high pilot overhead. To address this, the mapping entity employs an adaptive threshold method to constrain the pilot sequences, allowing only a limited number of pilot sequences to be transmitted at a given time. The formulation of limiting the pilot sequence based on the adaptive threshold method can be shown as

$$\begin{cases} \mathrm{Th}^1 < \mathrm{Ti}, \ \text{stop the } P; \\ \mathrm{Th}^2 \leqslant \mathrm{Ti} < \mathrm{Th}^1, \ \text{allow the } P \end{cases} \quad (19)$$

where Th^2 and Th^1 denote the upper and lower threshold levels respectively, Ti denotes the time of pilot sequence arrival. If the pilot sequence arrival crosses the lower threshold level, then the mapping entity constraints the pilot arrival and otherwise allows the pilot arrival.

Once the pilot arrival is constrained, the channel estimation is done using an ABPNN which estimates the channel state and encodes it in form of a channel vector based on metrics such as AoA, DoA, Time of arrival (ToA), channel gain, and environmental condition. The channel parameter description is provided as follows:

• **AoA.** The direction angle at where the signal is obtained by the mapping entity. The formulation of AoA can be provided as

$$\theta_{\mathrm{arrival}} = 180° - \theta_{\mathrm{zero}}^{\mathrm{sum}} + \theta_{\mathrm{pole}}^{\mathrm{sum}} \quad (20)$$

where $\theta_{\mathrm{arrival}}$ denotes the angle of arrival, $\theta_{\mathrm{zero}}^{\mathrm{sum}}$ is sum of zero angles, and $\theta_{\mathrm{pole}}^{\mathrm{sum}}$ is the sum of pole angles.

• **DoA.** The DoA is computed to determine at which direction the signal arrives from the entities to the mapping entity.

• **ToA.** The ToA is used to determine at which time the propagation signals are arrived at the mapping entity. The ToA estimation is highly essential for limiting the pilot signals.

• **Channel gain.** The channel gains are adopted to showcases the effects of shadowing, pathloss, and fading in the channel. The channel gain can be formulated as

$$Y = \mathrm{cG}X + \mathrm{noi} \quad (21)$$

where Y denotes the received signal, cG denotes the channel gain, X is the transmitted signal, and noi is noise in the signal.

• **Environmental conditions.** The uncertain environmental conditions also influence the channel estimation accuracy. The environmental conditions include the natural calamities which are also considered by the proposed work for robust channel estimation.

The ABPNN is composed of three layers such as input, hidden, and output layers, respectively. The adoption of maximization and minimization target value in the conventional BPNN provides the future output values to improve the estimation accuracy.

The input pilot signal can be denoted as

$$y\mathfrak{x}_z^{\mathrm{dl}} + y\mathfrak{x}_{z*}^{\mathrm{ul}} = yr \tag{22}$$

Then the input pilot signals are passed through the hidden layers. The hidden layer is composed of multiple neurons and activation functions for getting a hidden layer output that can be formulated as

$$\mathrm{hid}_i = \mathrm{act}_1\left(\sum_{j=1}^{n} \mathrm{we}_{ij}\mathrm{yr}_j - \mathrm{Th}_i\right) \tag{23}$$

where hid_i denotes the i-th hidden layer neuron, the activation function is denoted as act_1, and we_{ij} denotes the weight values among the neurons. The i-th neuron threshold can be denoted as Th_i. From the hidden layer, the computations are passed to the output layer which can be formulated as

$$\mathrm{op}_i = \mathrm{act}_2\left(\sum_{j=1}^{m} \mathrm{cwe}_{\mathrm{th},j}\mathrm{hid}_i - \mathrm{cwe}_{\mathrm{th}}\right) \tag{24}$$

where act_2 denotes the output activation function, and $\mathrm{cwe}_{\mathrm{th}}$ denotes the threshold of the connection weight among the neurons in the output layer. Once the output is obtained, the generated output is provided for adaptive forecasting of future output values. The formulation of adaptive forecasting can be expressed as

$$\widehat{\mathrm{op}}_{\mathrm{forecast}} = (\widehat{\mathrm{op}}_i + 1)(\max(\mathrm{op}_i) - \min(\mathrm{op}_i) + \min(\mathrm{op}_i)) \tag{25}$$

where $\widehat{\mathrm{op}}_{\mathrm{forecast}}$ denotes the forecasted output, $\max(\mathrm{op}_i)$ and $\min(\mathrm{op}_i)$ are the maximum and minimum target output respectively. After that, the forward propagation error can be formulated as

$$\mathrm{Err} = \frac{1}{2}\sum_{l}^{L}(\mathrm{op}_l - \mathrm{exop}_l)^2 \tag{26}$$

From Eq. (26), Err denotes the forward propagation error, op_l is the desired output from the output layer (i.e., obtained channel vector), and exop_l denotes the expected output. The estimated channel vector using ABPNN can be represented as $\mathfrak{p} = \mathrm{fwd}\left(\widehat{\mathrm{cV}}; \Xi_e\right)$ in which the $\mathfrak{p}$ denotes the low dimension vector, fwd(·) denotes the forward propagation operation, $\widehat{\mathrm{cV}}$ is the obtained channel vector, and Ξ_e denotes the parameter set for training the ABPNN. Finally, the error corrections at the hidden and output layers are separately provided. The error correction at the output layer can be formulated as

$$\vartheta_l = (\mathrm{exop}_l - \mathrm{op}_l)\mathrm{op}_l(1 - \mathrm{op}_l) \tag{27}$$

The error correction at the hidden layer can be formulated as

$$\mathrm{errc}_j = \left(\sum_{1}^{L} \mathrm{cwe}_{\mathrm{th},j} \times \mathrm{Err}\right)\mathrm{hid}_i(1 - \mathrm{hid}_i) \tag{28}$$

The estimated channel vectors are acknowledged to the transmitters and receivers. After some instance, the feedback is provided to the mapping entity in terms of achievable rate. Once the feedback is obtained, the channel quality is estimated by performing channel vector reconstruction. The channel reconstruction can be formulated as

$$\widehat{\mathrm{cV}}_{\mathrm{rcon}} = \mathrm{bwd}\left(\mathrm{fwd}\left(\widehat{\mathrm{cV}}; \Xi_e\right); \Xi_{\mathrm{rt}}\right) \tag{29}$$

where $\widehat{\mathrm{cV}}_{\mathrm{rcon}}$ is the reconstructed estimated channel, bwd(·) is the propagation unit, and Ξ_{rt} denotes the reconstruction training parameter. The reconstructed channel vector is quantized ($\mathfrak{Q}\left[\widehat{\mathrm{cV}}_{\mathrm{rcon}}\right]$) to achieve a robust HP design. Figure 3 and Algorithm 1 denote the machine learning based channel state estimation.

5.3 Data stream optimization & scheduling

Before designing the HPs/combiners, the data streams by the transmitters are optimized to achieve high SE. For that, the proposed work clustered the data streams into public and private streams using the EFCM algorithm based on metrics such as estimated channel state, and data stream similarity. The conventional FCM algorithm is enhanced by adopting Density Peaks Clustering (DPC) method. The DPC is used for cluster centre determination, and FCM is used for clustering the data streams into public and private data streams.

The data streams originating from the BS are denoted as $\mathrm{DS} = \{\mathrm{DS}_1, \mathrm{DS}_2, \ldots, \mathrm{DS}_n\}$. Using these data streams, the cluster center $\mathrm{clu}_{\mathrm{cen}}^j$ is calculated using the following formulas. Firstly, Eqs. (30) and (31) are used to compute the distance and local density, respectively.

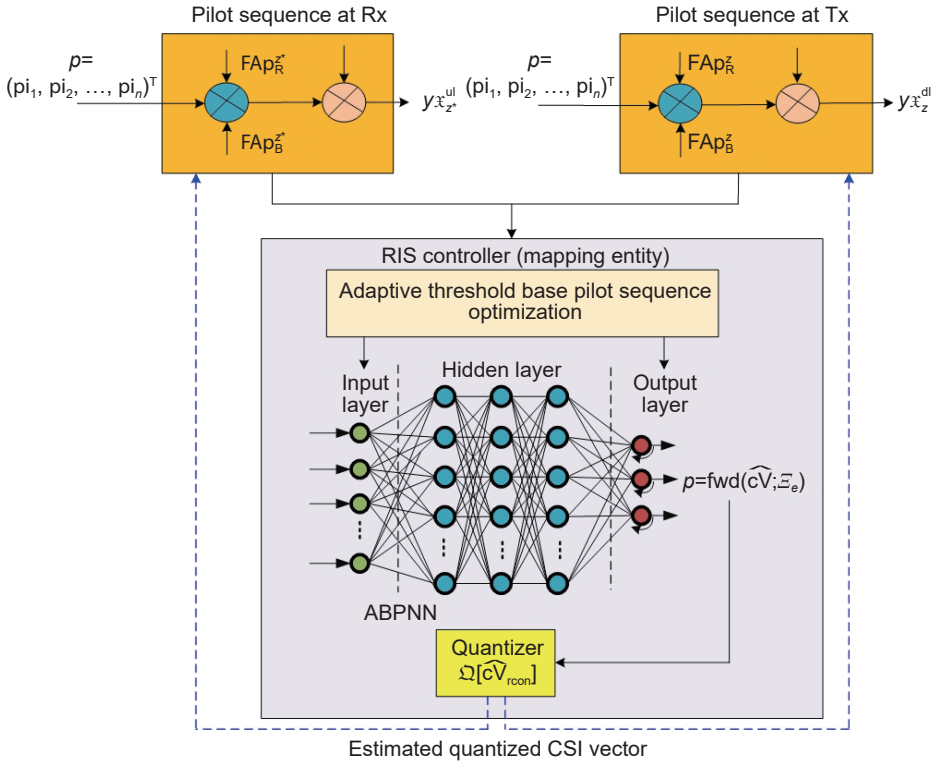

Fig. 3 Pilot optimization and machine learning based CSI estimation.

$$\tau_j = \min_{\varrho_j > \varrho_i} \left(\mathrm{Dis}_{ji}\right) \tag{30}$$

where Dis_{ji} denotes the distance between the j-th and i-th data stream, τ_j is the distance, and ϱ_j is the local density. ϱ_j can be formulated as

$$\varrho_j = \sum_i \xi\left(\mathrm{Dis}_{ji} - \mathrm{tru}_{\mathrm{dist}}\right) \tag{31}$$

where the sample distance between the j-th and i-th data stream can be denoted as Dis_{ji}, the truncation distance is denoted as $\mathrm{tru}_{\mathrm{dist}}$ in which $\xi(\varepsilon) = \begin{cases} 0, & \varepsilon \geqslant 0 \\ 1, & \varepsilon < 0 \end{cases}$. Once the cluster centers are determined, the index of the density value $\left(\mathfrak{y}_j\right)$ can be computed as

$$\mathfrak{y}_j = \varrho_j \tau_j \tag{32}$$

The density index value $\mathfrak{y}_j$ described above is applied to all the data streams to calculate their respective density indexes. These indexes are then sorted in descending order, and the top v streams are selected. The median density distance $\mathfrak{y}^{\mathrm{avg}}$ is then computed using these selected streams.

$$\mathfrak{y}^{\mathrm{avg}} = \frac{1}{v} \sum_{j=1}^{v} y_j \tag{33}$$

Data streams with $\mathfrak{y}_j > \mathfrak{y}^{\mathrm{avg}}$ based on the middling density distance are selected as cluster centers $\mathrm{clu}_{\mathrm{cen}}^{j}$. The cluster center matrix $\mathrm{clu}_{\mathrm{cen}}^{j} = \left\{\mathrm{clu}_{\mathrm{cen}}^{1}, \mathrm{clu}_{\mathrm{cen}}^{2}, \ldots, \mathrm{clu}_{\mathrm{cen}}^{j}\right\}$ and maximum iterations $(\mathrm{iter}_{\max})$ are also determined. The termination threshold $(\beth)$ and fuzzy index (two) are set, and the termination condition $\beth > 0$ is applied. The fuzzy membership matrix for each data stream is computed based on its distance from the cluster centre and the fuzzy objective function is calculated using the formula.

$$\Im(\mathfrak{U}, \mathfrak{V}) = \sum_{j=1}^{\mathcal{T}} \sum_{i=1}^{n} \left(\mathfrak{u}_{ji}\right)^n \left(D_{ji}^{\mathrm{Euc}}\right)^2 \tag{34}$$

From the above equation, $\mathcal{T}$ represents the number of fuzzy groups, n represents the number of samples (i.e., data streams) in the environment, $\mathfrak{U}$ and $\mathfrak{V}$ are the fuzzy membership functions and cluster centre group respectively. $\mathfrak{u}_{ji}$ is also the membership matrix of dimension $n \times \mathcal{T}$, and D_{ji}^{Euc} denotes the Euclidian distance among the normal data stream and the cluster center. After that, both the cluster center and membership matrix are updated by Eqs. (35) and (36) as

Algorithm 1 Machine learning based CSI estimation

Input: US pilot sequence ($y\text{x}_z^{\text{dl}}$), BS pilot sequence ($y\text{x}_{z*}^{\text{ul}}$)

Output: Quantized estimated channel vector $\Omega\left[\widehat{cV}_{\text{rcon}}\right]$)

Begin

Generate pilot sequence (Eqs. (17) and (18))

Pilot sequence → mapping entity (active elements)

Constrain the pilot sequence (Eq. (19))

If $\text{Th}^1 < \text{Ti}$ **then**

Stop the pilots received

Else

Receive the pilots

End If

For all the received pilots **do**

//Perform channel state estimation using ABPNN//

Obtain the CSI metrices

Provide the input pilot signal P (Eq. (22))

Provide P to the hid_i

Generate the output op_i channel vector ($p = \text{fwd}\left(\widehat{cV};\Xi_e\right)$)

Perform adaptive forecasting (Eq. (25))

Derive the forward propagation error (Eq. (26))

Perform error correction at output layer (Eq. (27))

Perform error correction at hidden layer (Eq. (28))

$p = \text{fwd}\left(\widehat{cV};\Xi_e\right)$ → mapping entity (active elements)

Obtain feedback from US and BS

Reconstruct the channel vector (Eq. (29))

Quantize the reconstructed channel $\Omega\left[\widehat{cV}_{\text{rcon}}\right]$

End For

End

$$\mathfrak{V}_j = \frac{\sum_{i=1}^{n}\left(\mathfrak{u}_{ji}\right)^n \text{DS}_j}{\sum_{i=1}^{n}\left(\mathfrak{u}_{ji}\right)^n} \tag{35}$$

$$\mathfrak{u}_{ji} = \begin{cases} 1 \\ \dfrac{1}{\sum_{k=1}^{\mathcal{T}} \dfrac{D_{ji}^{\text{Euc}}}{D_{ki}^{\text{Euc}}}^{\frac{1}{n-2}}} \end{cases} \tag{36}$$

The above process of updation will be continued untill condition for maximum iteration met or computed error is smaller than the $\beth$, whereas the updation continues untill its forms the desired clusters into two types as public and private data streams. The data stream clusters can be expressed as

$$\text{Clus} = \begin{bmatrix} \text{pub}_{\text{DS}}^{\text{Clu}} = \left(\text{pub}_1^{\text{Clu}}, \text{pub}_2^{\text{Clu}}, \ldots, \text{pub}_n^{\text{Clu}}\right), \\ \text{pri}_{\text{DS}}^{\text{Clu}} = \left(\text{pri}_1^{\text{Clu}}, \text{pri}_2^{\text{Clu}}, \ldots, \text{pri}_n^{\text{Clu}}\right) \end{bmatrix} \tag{37}$$

The scheduling of data streams in both public and private time scales is based on their priority and emergency levels. The priority level indicates the importance of a data stream relative to others, while the emergency level indicates the urgency or time sensitivity of a data stream. The scheduling technique is defined by Eq. (38), where Y is the scheduling constant, $\text{Ti}_1 S\left[\text{pub}_{\text{DS}}^{\text{Clu}}\right]$ represents the time scale of public streams, and $\text{Ti}_2 S\left[\text{pri}_{\text{DS}}^{\text{Clu}}\right]$ represents the time scale of private data streams. The public and private data streams perform transmission, idle, and reception, depending on the RF one-bit DAC/ADC's capability in the precoder and combiner, respectively. The proposed scheduling process is further illustrated in Algorithm 2 and Fig. 4.

$$Y = \begin{cases} \text{Ti}_1 S\left[\text{pub}_{\text{DS}}^{\text{Clu}}\right] = \{\text{transmit}, \text{idle}, \text{receive}\}, \\ \text{Ti}_2 S\left[\text{pri}_{\text{DS}}^{\text{Clu}}\right] = \{\text{transmit}, \text{idle}, \text{receive}\} \end{cases} \tag{38}$$

5.4 Cooperative HP design

The HP design is a crucial task that involves jointly optimizing the one-bit DAC-RF chain pairs on the transmitter side and adjusting the position of the vector modulated phase shifters in the DHRR-RIS. To achieve this, the scheduled data streams and estimated channel vectors are provided as input to the DRL agent, which uses the DDPG algorithm for optimization. Additionally, the position of the vector modulated phase shifters in the DHRR-RIS is adjusted using the FHO algorithm. To ensure design accuracy, the Mean Square Error (MSE) must be reduced, and hence the problem is formulated as cooperative.

The proposed cooperative optimization of HP can be formulated as

$$\begin{aligned} &\min_{\{F_{\text{DP}}, F_{\text{AP}}, \varpi, \mathfrak{u}\}} \text{MSE}, \\ &\text{Such that}: \; c_1 : F_{\text{AP}} \in f, c_2 : \varpi \in \mathfrak{r}, \\ &c_3 : \|F_{\text{AP}} F_{\text{DP}}|_F^2 = A, c_4 : \mathfrak{u} \in G_+ \end{aligned} \tag{39}$$

From the above problem formulation, F_{AP}, F_{DP}, ϖ, and $\mathfrak{u}$ represent the analog precoder at the DHRR-RIS, digital precoder at BS, vector modulated phase shifter matrix, and DHRR-RIS controller gain, respectively.

5.4.1 Digital precoder design on transmitter side

The DRL algorithm optimizes the digital precoder F_{DP}

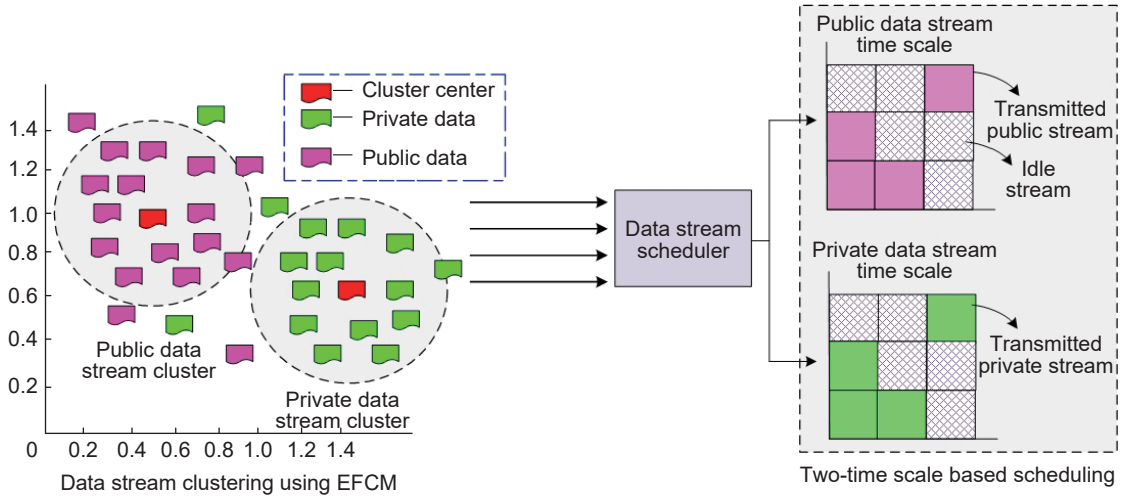

Fig. 4 EFCM-based data stream clustering and two-time scale based scheduling.

Algorithm 2 Data stream optimization & scheduling

Input: Data streams (DS) and cluster centers ($\mathrm{clu}_{\mathrm{cen}}^{j}$)
Output: Data stream clusters (Clus) and scheduling (Y)
Begin
Initialize the DS = $\{\mathrm{DS}_1, \mathrm{DS}_2, \ldots, \mathrm{DS}_n\}$
For all DS **do**
//Determine the $\mathrm{clu}_{\mathrm{cen}}^{j}$*//*
Compute τ_j and ϱ_j (Eqs. (30) and (31))
Determine the density index value $\mathfrak{y}_j$ (Eq. (32))
Compute the middling density distance $\mathfrak{y}^{\mathrm{avg}}$ (Eq. (33))
If $\mathrm{DS}^j = \mathfrak{y}_j > \mathfrak{y}^{\mathrm{avg}}$ **then**
DS^j is selected as a cluster
Else Normal DS^j
End If
Form $\mathrm{clu}_{\mathrm{cen}}^{j} = \left\{\mathrm{clu}_{\mathrm{cen}}^{1}, \mathrm{clu}_{\mathrm{cen}}^{2}, \ldots, \mathrm{clu}_{\mathrm{cen}}^{j}\right\}$
End For
Initialize $\mathrm{clu}_{\mathrm{cen}}^{j}$, $\mathrm{iter}_{\max}$, ⊐, fuzzy index=2
Formulate the fuzzy objective function $\mathfrak{J}(\mathfrak{U}, \mathfrak{V})$
For all fuzzy groups **do**
Update $\mathfrak{V}_j$ and $\mathfrak{u}_{ji}$ until error < ⊐
If error < ⊐ **then**
Stop and exit
Else Continue updation
End If
Form clusters Clus
End For
Perform two level scheduling for Clus (Eq. (38))
End

by jointly optimizing the one-bit DAC-RF chain pairs on the transmitter side using DDPG. This reduces the number of active transmitters, thereby improving antenna gain. The DRL algorithm is chosen because it adapts its processes based on the environment state. The DDPG is an actor-critic model that learns both the actor ($И_ü$) and critic ($Þ_ë$) functions. The parameters of the DDPG include state (St), action (Ac), reward (Re), state-action pair (St, Ac), discount factor (∇), and condition for termination. Table 3 summarizes the functions of these three main parameters in digital precoder design.

Given the present condition of the environment, represented by the estimated channel vector $\Omega\left[\widehat{\mathrm{cV}}_{\mathrm{rcon}}\right]$, and the scheduled data streams Y, a DRL entity selects an action to optimize the DAC-RF pairs in the digital precoder. To achieve this optimization, the entity uses the previous states of $F_{\mathrm{AP}}^{(t-1)}$ and $\varpi^{(t-1)}$ obtained from the reply buffer at the previous timestamp. By adhering to the minimum MSE minimization problem (Eq. (39)), the digital precoder optimization can be formulated as

$$F_{\mathrm{DP}}^{(t)} = \left[\mathfrak{h}^{(t)}\left(F_{\mathrm{AP}}^{(t-1)}\right)^{\mathrm{CM}} F_{\mathrm{AP}}^{(t-1)}\right]^{-1}\left(\mathrm{CM}^{(t-1)} F_{\mathrm{AP}}^{(t-1)}\right)^{\mathrm{CM}} \quad (40)$$

The optimization constant $\mathfrak{h}^{(t)}$ determines the activation and deactivation of DAC-RF chain pairs based on their capacity and capability, while

Table 3 Parameters of proposed DDPG.

Parameter	Description
State (St)	Scheduled data streams and the estimate channel vectors at the current time stamp
Action (Ac)	Performs optimization of DAC-RF pairs by performing on and idling them
Reward (Re)	Reduced MSE with high SE and achievable rate

$\left(F_{\mathrm{AP}}^{(t-1)}\right)^{\mathrm{CM}}$ represents the estimated channel between DP and AP (i.e., DHRR-RIS) at the previous timestamp, where CM is the channel matrix between the BS and DHRR-RIS. The actor and critic networks are updated through stochastic gradient descent using two loss functions. The mini-batches of samples $\{\mathrm{st}_i, \mathrm{ac}_i, \mathrm{ter}_i, \mathrm{st}_{i+1}\}$ are used to extract the loss functions, where $\mathrm{ter}_i = \mathrm{ter}(\mathrm{st}_i, \mathrm{ac}_i)$ is the termination condition index and st_{i+1} denotes the state transition. The target networks, $И_{ü'}$ and $Þ_{ë'}$, composed of actor and critic networks, respectively, are used to maintain stability in the DDPG network and approximate function. The update losses for the actor and critic can be expressed as

$$\mathrm{Loss}_{ü} = -\sum_i Þ_{ë}(\mathrm{st}_i, И_{ü}(\mathrm{st}_i)) \tag{41}$$

$$\mathrm{Loss}_{ë} = \sum_i [Þ_{ë}(\mathrm{st}_i, \mathrm{ac}_i) - \propto_i]^2 \tag{42}$$

where $\propto_i$ is the reward function formulation based on the state transitions in the target state-action space which is expanded as $\propto_i = \mathrm{Re}_i + \nabla(1-\mathrm{ter}_i)Þ_{ë'}(\mathrm{st}_{i+1}, И_{ü'}(\mathrm{st}_{i+1}))$. Algorithm 3 represents the DRL-based digital precoder design at the transmitter side.

5.4.2 Analog precoder design at the DHRR-RIS

The RIS entity employs the FHO algorithm to adjust the position of the vector modulated phase shifters (i.e., analog precoder F_{AP}) in the DHRR-RIS for optimal performance. Using information obtained from the DRL entity, the proposed analog precoder is designed. The two entities work cooperatively to achieve a robust, energy-efficient HP design. FHO is adopted for analog precoder design due to its ability to provide an optimal solution with high convergence and learning rates and without getting trapped in local optima. In this work, the vector modulated phase shifters of the passive elements are treated as fire hawks. Initially, the position vectors of the passive elements in the DHRR-RIS are initialized as

$$\mathrm{VM}_{\mathrm{ps}} = \begin{bmatrix} \mathrm{VM}_{\mathrm{ps}_1} \\ \mathrm{VM}_{\mathrm{ps}_2} \\ \vdots \\ \mathrm{VM}_{\mathrm{ps}_N} \end{bmatrix} = \begin{bmatrix} \mathrm{VM}_{\mathrm{ps}_1}{}^{1} & \mathrm{VM}_{\mathrm{ps}_1}{}^{2} & \cdots & \mathrm{VM}_{\mathrm{ps}_1}{}^{d} \\ \mathrm{VM}_{\mathrm{ps}_2}{}^{1} & \mathrm{VM}_{\mathrm{ps}_2}{}^{2} & \cdots & \mathrm{VM}_{\mathrm{ps}_2}{}^{d} \\ \vdots & \vdots & \ddots & \vdots \\ \mathrm{VM}_{\mathrm{ps}_N}{}^{1} & \mathrm{VM}_{\mathrm{ps}_N}{}^{2} & \cdots & \mathrm{VM}_{\mathrm{ps}_N}{}^{d} \end{bmatrix} \tag{43}$$

To be more specific,

$$\mathrm{VM}_{\mathrm{ps}^j}^{i}(0) = \mathrm{VM}_{\mathrm{ps}^j,\min}^{i} + \mathrm{RAN}\left(\mathrm{VM}_{\mathrm{ps}^j,\max}^{i} - \mathrm{VM}_{\mathrm{ps}^j,\min}^{i}\right) \tag{44}$$

The variable d represents the dimension of the problem, and the total number of solution vectors is denoted as N. $\mathrm{VM}_{\mathrm{ps}^j}^{i}$ represents the j-th solution passive element vector of the DHRR-RIS, while $\mathrm{VM}_{\mathrm{ps}^j,\max}^{i}$ and $\mathrm{VM}_{\mathrm{ps}^j,\min}^{i}$ represent the maximum and minimum bounds of the j-th passive element, respectively. Objective functions are determined based on the distance and channel condition between the passive element and BS. The passive element with the least distance and path loss is given a higher objective function (i.e., global best passive element), while other passive elements with a considerable distance and path loss are considered the best passive element. The distance between the passive element and BS can be formulated as

$$\mathrm{Dis}_k^u = \sqrt{(y_2-y_1)^2 + (x_2-x_1)^2}, \begin{cases} k = 1,2,\ldots,m; \\ u = 1,2,\ldots,s \end{cases} \tag{45}$$

where Dis_k^u is the distance among the u-th passive vector modulated phase shifter and the k-th BS, the (y_2-y_1) and (x_2-x_1) is the vector modulated phase shifters and BS co-ordinates in the environment respectively. In similar manner, the path loss among

Algorithm 3 DRL-based digital precoder design

Initialize the actor ($И_{ü}$) and critic ($Þ_{ë}$) functions
Initialize the target network function $И_{ü'}$ and $Þ_{ë'}$
Set the reply buffer Ð
For Episode=1, **do**
  Perform action exploration by process initialization
  Perform observation of the initial state (st)
  For ter=1, $\mathrm{ter}_{\max}$ **do**
    Pick the action based on the current policy $И_{ü}$
    Act of F_{DP} optimization (Eq. (40)) and observer Re
    Store $[\mathrm{st}_{i+1}] \rightarrow$ Ð
    Set the $\propto_i = \mathrm{Re}_i + \nabla(1-\mathrm{ter}_i)Þ_{ë'}(\mathrm{st}_{i+1}, И_{ü'}(\mathrm{st}_{i+1}))$
    Actor policy updation by minimizing $\mathrm{Loss}_{ü}$ (Eq. (41))
    Critic policy updation by minimizing $\mathrm{Loss}_{ë}$ (Eq. (42))
    Perform updation of target networks $И_{ü'}$ and $Þ_{ë'}$
  End For
End For

the u-th vector modulated phase shifter and k-th BS can be formulated as

$$\mathrm{PL} = 10 \times \log\left(\frac{4\pi p_{\mathrm{d}}}{\lambda}\right)^2 - \mathrm{GA_r} - \mathrm{GA_{DHRR-RIS}} \tag{46}$$

where λ denotes the path loss, p_{d} is the distance of the path length, $\mathrm{GA_{DHRR-RIS}}$ is the gain of the antenna in DHRR-RIS, and $\mathrm{GA_r}$ is the gain of antennas in the BS. Based on the Dis_k^u and PL the objective function of the analog precoder design can be formulated as

$$\mathrm{obj}(F_{\mathrm{AP}}) = \begin{cases} \mathrm{VM_{ps}} \rightarrow \mathrm{less}\left(\mathrm{Dis}_k^u\right) \\ \mathrm{VM_{ps}} \rightarrow \mathrm{less}\left(\mathrm{PL}\right) \end{cases} \tag{47}$$

Based on the objective function of the analog precoder $\mathrm{obj}(F_{\mathrm{AP}})$ and the obtained $F_{\mathrm{DP}}^{(t)}$, the optimization of the analog precoder can be determined. If the objective function of the passive element is high then the passive element is more likely to be optimized otherwise, the next passive element with high objective function is selected from above constrains (Eq. (44)). In addition to that, the problem of minimum mean squared error also minimized by

$$F_{\mathrm{AP}}^{(t)} = \left[\mathrm{obj}(F_{\mathrm{AP}})\left(F_{\mathrm{DP}}^{(t-1)}\right)^{\mathrm{CM}} F_{\mathrm{DP}}^{(t-1)}\right]^{-1}\left(\mathrm{CM}^{(t-1)} F_{\mathrm{DP}}^{(t-1)}\right)^{\mathrm{CM}} \tag{48}$$

where the objective function $\mathrm{obj}(F_{\mathrm{AP}})$ is obtained from the FHO algorithm, which determines the optimization of the passive elements in the DHRR-RIS. The phase shifter matrix ϖ is then optimized using the gradient projection method while considering the MSE minimization constraint. Finally, the proposed hybrid precoding approach (i.e., DRL-based digital precoding & FHO-based analog precoding) is utilized to realize hybrid beamforming, where the beams are reflected by the adjusted passive elements to the receivers. On the receiver side, the combiner is designed based on the DA-DDPG, and the one-bit ADC-RF chain pairs are optimally adjusted to fully utilize the transmitted beams without hardware complexity. The pseudocode for FHO-based analog precoder design at the DHRR-RIS is provided in Algorithm 4 for a better understanding.

Algorithm 4 FHO-based analog precoder design

Input: $F_{\mathrm{DP}}^{(t)}$, Initial population vector of passive elements

Output: $F_{\mathrm{AP}}^{(t)}$ optimized analog precoder

Begin

Initialize the position vectors of the passive elements (Eq. (44))

// Objective function determination //

Compute the distance among passive element and BS Dis_k^u (Eq. (45))

Compute the path loss PL (Eq. (46))

Obtain the objective function $\mathrm{obj}(F_{\mathrm{AP}})$ (Eq. (47))

If $\mathrm{obj}(F_{\mathrm{AP}})$ is high **then**

Perform analog precoder optimization (Eq. (48))

Else

Another passive element is selected based on (Eqs. (43) and (48))

End If

End

6 Experimental result

This section presents the analysis of experimental results of the proposed and prior works. The experimental results analysis section is composed of four sub-sections, namely simulation set-up, comparative analysis, complexity analysis, and research summary. Further details of all supplementary sections are provided below.

6.1 Experimental setup

The proposed DHRR-RIS based HP design model was implemented and simulated using the MATLAB R2020a tool. The simulation process involved designing a Simulink model, running the model to obtain QAM results based on pilot signals, machine learning-based CSI estimation, clustering-based data stream optimization and scheduling, and cooperative HP design. The proposed work achieves better results by optimally configuring the system settings. The software configuration of the system includes the Windows 10 operating system and the MATLAB R2020a simulation tool. The hardware configuration of the system included a 1-terabyte hard disk, an Intel(R) Core(TM) i5-4590S CPU @ 3.00 GHz processor, and 6 GB of RAM. To better understand the simulation results, a visual representation of the results is shown in Figs. 5−9.

Figure 5 depicts the Simulink model utilized for the proposed simulation, while Fig. 6 presents the clustering results obtained using the proposed method

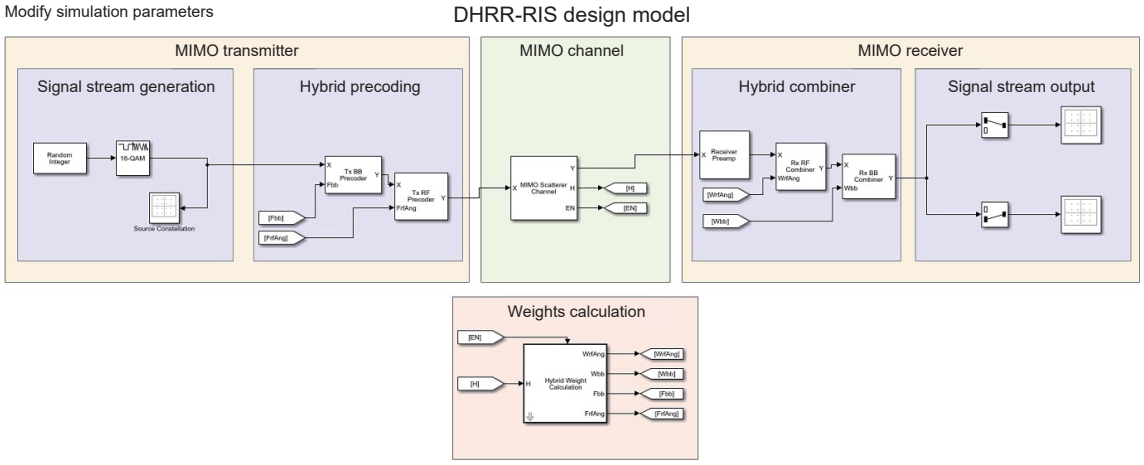

Fig. 5 Simulink model.

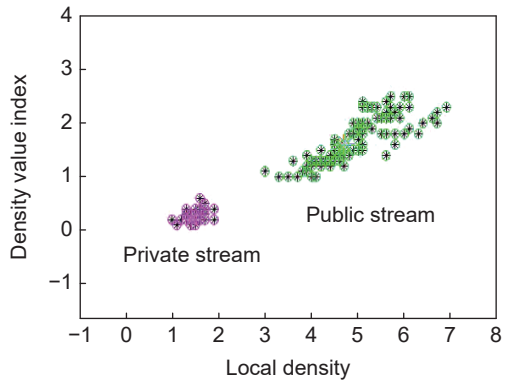

Fig. 6 Clustering results.

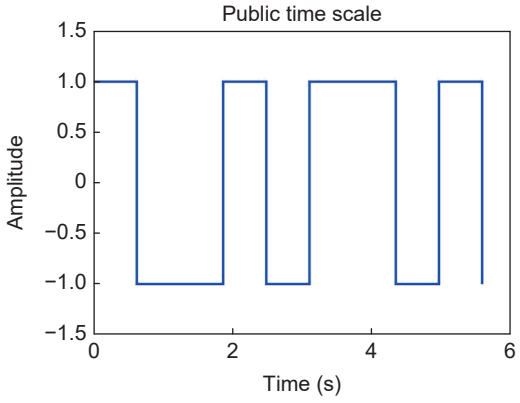

Fig. 7 Public data stream scheduling.

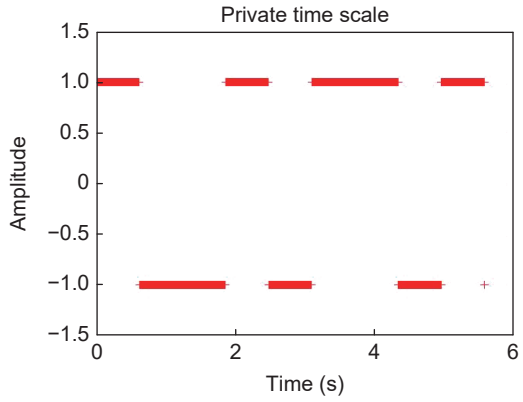

Fig. 8 Private data stream scheduling.

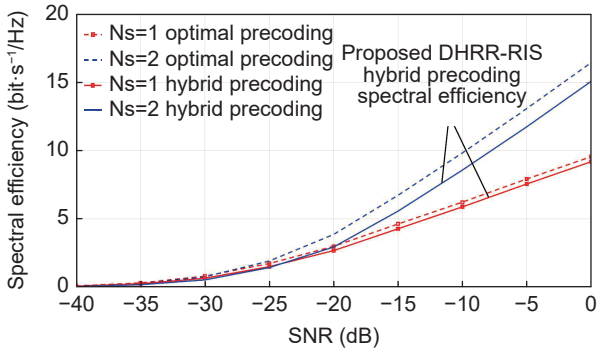

Fig. 9 Hybrid precoding results.

to distinguish between public and private data streams.

Furthermore, Fig. 7 displays the scheduling outcomes of private data streams, whereas Fig. 8 portrays the scheduling outcomes of public data streams. Lastly, Fig. 9 illustrates the results of the hybrid precoding, indicating that the proposed method attains higher SE.

6.2 Comparative analysis

This section presents a comparative analysis of the proposed HP-DHRR-RIS method against select state-of-the-art techniques, including Reconfigurable Intelligent Surface based Hybrid Precoding (RIS-HP)[21], Double Reconfigurable Intelligent Surface based Hybrid Precoding (DRIS-HP)[22], and

Convolutional Neural Network based Hybrid Precoding (CNN-HP)[30]. Validation metrics, including SE, WSR, and BER are employed for the purpose of comparison.

6.2.1 WSR analysis

The WSR is a crucial metric for communication systems utilizing MU-MIMO technology, as it enables control over power, network, and utility maximization within the environment. This metric prioritizes users optimally, with the aim of maximizing the overall system performance. For an effective system, the WSR must be maximized. The analysis of WSR is further divided into three scenarios, which are explained below.

WSR based on reflecting elements in DHRR-RIS

The passive reflecting elements are responsible for analog beamforming in the proposed environment. Therefore, it is crucial to properly adjust these elements to achieve a higher WSR.

Figure 10 depicts the WSR analysis for varying numbers of reflecting elements. It is observed that the WSR increases with an increase in the number of reflecting elements. The proposed method achieves a higher WSR than existing techniques, as it utilizes an optimization-based approach for adjusting the reflecting elements in intelligent surfaces. Specifically, the proposed method adopts the DHRR-RIS passive element as the analog beamformer for achieving hybrid precoding. To achieve this, the proposed method optimizes the position of vector modulated phase shifters in the passive elements using the FHO algorithm based on the distance between the DHRR-RIS and transmitter, as well as the path loss between them. By optimally adjusting the reflecting elements in the DHRR-RIS, the proposed method maximizes the WSR. Conversely, the existing RIS-HP method maximizes the sum rate by adopting a deep learning algorithm. However, its lack of consideration of optimal metrics for analog precoding results in a lower WSR compared to the proposed method. The DRIS-HP technique utilizes the RMO algorithm for phase shift optimization but has a higher computational complexity, which hinders its WSR.

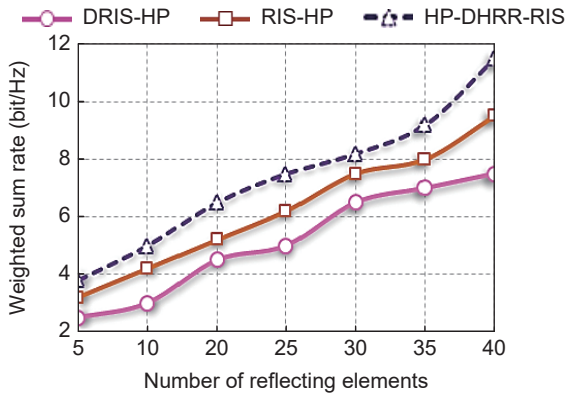

Fig. 10 Number of reflecting elements vs. WSR.

Based on the numerical results of the WSR analysis in relation to the number of reflecting elements in the RIS, the proposed method achieves a higher WSR of 11.5 bit/Hz when the number of reflecting elements reaches 40. In contrast, existing techniques such as RIS-HP and DRIS-HP limit the WSR to 9.5 bit/Hz and 7.5 bit/Hz, respectively, for the same number of reflecting elements. This demonstrates that the proposed method outperforms existing techniques with a difference of 2 bit/Hz to 4 bit/Hz higher WSR.

WSR based on transmitter and receiver antenna

This section presents a comparison of the proposed HP-DHRR-RIS with existing works in terms of the WSR analysis based on transmitter and receiver antennas in the BS and Us. The optimization and balancing of both antennas are crucial for effective communication in the proposed environment.

Figures 11 and 12 graphically illustrate the comparison of WSR to transmitter and receiver antennas. The proposed work achieves higher WSR than the existing works because it optimizes both antennas by switching the pairs of RF chains DAC/ADC between on and idle modes based on incoming/outgoing streams and the capability and capacity of the RF-DAC/ADC pairs. This reduces energy wastage and complexity during transmission and reception, thereby increasing WSR. In contrast, the existing works RIS-HP, DRIS-HP, and CNN-HP do not consider the complexity and energy wastage in the transmitter and receiver antennas, limiting their WSR.

The numerical results of the WSR analysis with the transmitter antenna show that the proposed work achieves a higher WSR of 5.8 bit/Hz when the number

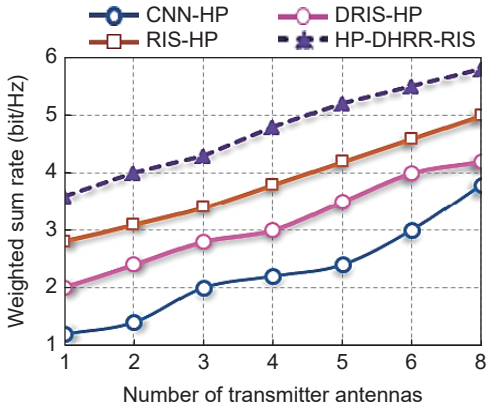

Fig. 11 Number of transmitter antennas vs. WSR.

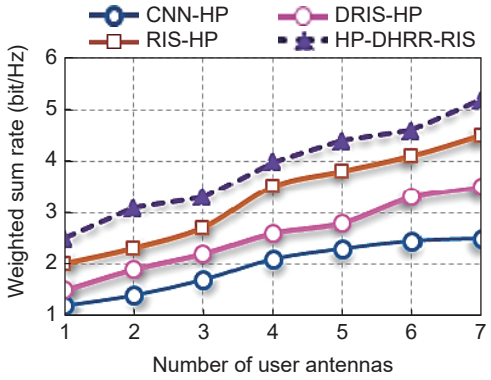

Fig. 12 Number of user antennas vs. WSR.

of transmitter antennas increases to 8. In contrast, the existing works RIS-HP, DRIS-HP, and CNN-HP achieve a lesser WSR of 5 bit/Hz, 4.2 bit/Hz, and 3.8 bit/Hz, respectively, for the same number of transmitter antennas. The proposed work achieves a difference of 0.8−2 bit/Hz higher than the existing works.

The numerical results of the WSR with receiver antennas show that when the number of receiver antennas increases to 7, the WSR of the proposed work increases to 5.2 bit/Hz. For the same number of receiver antennas, the existing works RIS-HP, DRIS-HP, and CNN-HP achieve a lesser WSR of 4.5 bit/Hz, 3.5 bit/Hz, and 2.5 bit/Hz, respectively. The difference between the proposed and existing works is 0.7−2.7 bit/Hz higher.

6.2.2 BER analysis

BER is an important performance metric that measures the accuracy of the communication system by evaluating the number of erroneous bits transmitted over a channel with respect to the total number of transmitted bits. A lower BER indicates better performance and higher quality of the communication system. BER is affected by various factors such as signal-to-noise ratio, modulation scheme, channel conditions, and interference.

BER based on RF-DAC/ADC pairs

The RF-DAC/ADC pairs are crucial components residing in the digital precoder and combiner of the BS and US, respectively, responsible for baseband communication and signal conversion of the raw data streams. To minimize the BER, proper handling of the RF-DAC/ADC pairs is essential.

Figure 13 presents a comparison of the BER to RF-DAC/ADC pairs. The results indicate that an increase in the number of RF-DAC/ADC pairs leads to a higher BER. This is due to the high noise and interference levels present in the many incoming and outgoing data streams. However, the proposed work achieves a lower BER than previous works. The proposed method performs channel estimation using a machine learning algorithm during transmission and reception, which is based on metrics such as AoA, ToA, DoA, channel gain, and environmental conditions. By performing machine learning-based channel estimation before transmission and reception, the incoming/outgoing data stream bits are free from noise, thereby reducing the BER. Conversely, previous works such as RIS-HP, DRIS-HP, and CNN-HP lack channel state estimation and focus solely on HP design, resulting in a higher BER and reduced beamforming efficacy.

The numerical results of the BER with a varying number of RF-DAC/ADC pairs indicate that, with eight RF-DAC/ADC pairs, the proposed work achieves

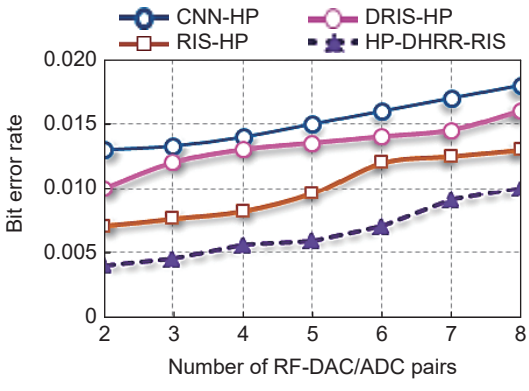

Fig. 13 Number of RF-DAC/ADC pairs vs. BER.

a BER of 0.01. In contrast, for the same number of RF-DAC/ADC pairs, the existing works RIS-HP, DRIS-HP, and CNN-HP have higher BERs of 0.013, 0.016, and 0.018, respectively. The proposed method exhibits a difference of 0.003−0.007 lesser than the previous works, indicating its superiority in BER reduction.

BER based on pilots

Pilot signals are commonly used in communication systems for synchronization, reference, continuity, equalization, etc. Therefore, effective handling of pilot signals is necessary to reduce unwanted BER in the system.

Figure 14 compares the proposed and existing BER with the number of pilot signals. In contrast to other graphical analyses, an increase in the number of pilots leads to a decrease in BER. This is because a lower number of pilots reduces their utilization rate, while a higher number of pilot signals increases their utilization rate for the intended purpose. Among the different methods, the proposed work achieves a lower BER than the existing works. This is because the proposed work limits the rate of pilot signal transmission, as excessive or less transmission affects communication reliability and leads to an increase in BER.

The proposed work employs an adaptive threshold method to limit the incoming pilots, thereby increasing communication reliability and reducing BER. In contrast, the existing works RIS-HP, DRIS-HP, and CNN-HP lack a pilot transmission limiting mechanism, which leads to deprived communication reliability and higher BER.

The numerical results of BER with the number of pilots show that when the pilot transmission rate increases to 50, the proposed work achieves a BER of 0.01. For the same number of pilots, the existing works RIS-HP, DRIS-HP, and CNN-HP achieve higher BER of 0.013, 0.024, and 0.029 11, respectively. The difference between the proposed and existing works is 0.03−0.2711 lesser.

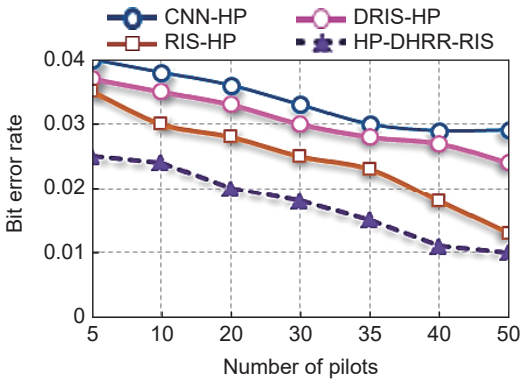

Fig. 14 Number of pilots vs. BER.

6.2.3 SE analysis

SE, defined as the ratio of channel bit rate and channel spacing, is an important metric for analyzing the amount of data that can be transmitted/received over a given bandwidth. In Fig. 15, we compare the SE of our proposed method to that of existing approaches for varying numbers of data streams.

The results demonstrate that as the number of data streams increases, the SE also increases. Our proposed method achieves higher SE than prior works due to our focus on data stream optimization and scheduling. Specifically, we employ the EFCM algorithm to cluster data streams into private and public groups based on their similarity level and channel estimation results, respectively. These clustered data streams are then scheduled into two-time scales based on their priority level. By optimizing data streams at the BS side, we reduce the chance of complexity due to over-transmission and increase the SE. In contrast, existing works such as RIS-HP, DRIS-HP, and CNN-HP do not focus on optimizing data streams, leading to higher complexity and decreased SE.

The numerical results show that our proposed method achieves an SE of 33 (bit/s)/Hz with 15 data streams, while RIS-HP, DRIS-HP, and CNN-HP

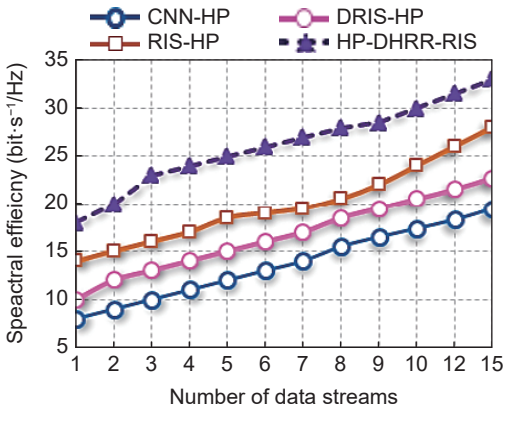

Fig. 15 Number of data streams vs. SE.

achieve 28 (bit/s)/Hz, 22.7 (bit/s)/Hz, and 19.5 (bit/s)/Hz, respectively. The difference between our proposed method and existing works is 5−14.5 (bit/s)/Hz higher.

6.3 Complexity analysis

In this section, we analyze the computational complexity of the proposed work. The proposed approach reduces computational complexity by implementing intelligent and lightweight processes in the MU-MIMO environment. The computational complexities of each process are summarized below.

The CSI estimation based on the ABPNN algorithm has a computational complexity of $O\left(A_{\mathrm{r}}^{5}A_{\mathrm{t}}\right)$, where A_{r} and A_{t} denote the number of receiver and transmitter antennas, respectively.

The computational complexity of data stream clustering and scheduling using the EFCM algorithm is $O(\mathrm{li_N clu_N iter}) + O\left(nc^2\right)$, where $\mathrm{li_N}$ denotes the total links, $\mathrm{clu_N}$ denotes the cluster links (set to 2), iter denotes the number of iterations, n denotes the number of clustered data streams to be scheduled, and c^2 represents the constraints for scheduling.

The cooperative hybrid precoding design includes DRL-based (i.e., DDPG) digital precoder design and metaheuristics-based (i.e., FHO) analog precoder design. The computational complexity of DDPG-based digital precoder design is $O\left(\mathrm{St}^2\mathrm{Ac}^2E\right)$, where St^2 represents the state, Ac^2 represents the action, and E represents the number of episodes. The computational complexity of FHO-based analog precoder design is $O(3\times\dim\times\mathrm{VM_{ps}}\times\mathrm{iter})\times O(\mathrm{obj}(F_{\mathrm{AP}}))$, where dim represents the dimensions, $\mathrm{VM_{ps}}$ represents the variable metric procedure size, iter denotes the number of iterations, and $\mathrm{obj}(F_{\mathrm{AP}})$ denotes the objective function.

Overall, the computational complexity of the proposed DHRR-RIS-based low complexity HP design using AI algorithms can be expressed as $O(A_{\mathrm{t}}^{5}A_{\mathrm{r}} + \mathrm{li_N clu_N iter} + nc^2 + \mathrm{St}^2\mathrm{Ac}^2E + 3\times\dim\times\mathrm{VM_{ps}}\times\mathrm{iter} + \mathrm{obj}(F_{\mathrm{AP}}))$.

6.4 Research summary

The summary section briefs the simulation results analysis of the proposed and existing works respectively. Based on the simulation results, the proposed research performs a comparative analysis of the proposed work with best picked existing works in terms of several validation metrics. The graphical and theoretical comparisons are shown in Figs. 10−15. The numerical comparisons are shown in Table 4. All the results show the proposed work outperforms the existing works. The major highlights of the proposed work are emphasized below.

• For reducing the channel estimation errors, we constrain the pilot transmission of the transmitter based on the adaptive threshold method. Further, the channel estimation is done at the DHRR-RIS side to use the ABPNN algorithm to reduce the estimation errors and computation overhead.

• For achieving high SE, we perform data stream optimization in which the transmitter data streams are clustered using EFCM as private and public clusters, and the clusters are scheduled into two-time scales to reduce the complexity during design.

• For reducing the hardware impairments and root mean phase error loss, we adopt one-bit DAC/ADC for the transmitter and receiver digital precoder side, and vector modulated phase shifters for the analog precoder and combiner side.

• To ensure theHP/combiner design robustness, we perform joint DRL (DA-DDPG)- and FHO-based

Table 4 Comparison of proposed and existing works results.

Metric vs. validator		CNN-HP	DRIS-HP	RIS-HP	Proposed HP-DHRR-RIS	Difference
WSR (bit/Hz)	Reflecting element	3.8	5.14	6.25	7.38	1.13−3.58
	Transmitter antenna	2.285	3.128	3.842	4.74	0.898−2.455
	Receiver antenna	1.95	2.542	3.271	3.871	0.6−1.921
BER	RF-DAC/ADC pair	0.0151	0.0132	0.0099	0.0065	0.0034−0.0086
	Pilot	0.0335	0.030	0.024	0.017	0.007−0.0165
SE (bit·s^{-1}/Hz)	Data stream	13.69	16.65	19.96	26.17	6.21−12.48

cooperative optimization of RF-DAC/ADC pairs of the HP/combiner and phase shifters using the DRL entity and RIS entity.

7 Conclusion

The RIS-based HP design for MIMO systems faces challenges such as energy consumption, channel estimation errors, and reduced SE. To address these issues, this proposed work utilizes DHRR-RIS and AI technologies. DHRR-RIS reduces computational complexity and allows for resilient scalability. The proposed system includes entities such as Us, BS, and RIS controllers, which consist of sub-entities such as the mapping entity, optimization entity, DRL entity, and RIS entity. The DHRR-RIS model is designed with vector modulated phase shifters in the passive elements. Pilot optimization and CSI estimation are performed using the adaptive threshold method and ABPNN algorithm. Transmitter data streams are optimized by clustering and scheduling into public and private data streams using the EFCM algorithm. Finally, cooperative HP design is performed by jointly optimizing one-bit DAC pairs in the BS side and reflecting elements in the DHRR-RIS side using DDPG and FHO algorithms. The proposed work is tested and implemented in the simulation environment using MATLAB R2020a with strong system configurations. The proposed work outperforms existing works in terms of validation metrics such as SE, WSR, and BER.

References

[1] A. S. Gharagezlou, M. Nangir, N. Imani, and E. Mirhosseini, Energy efficient power allocation in massive MIMO systems with power limited users, in *Proc. 4th Int. Conf. Telecommunications and Communication Engineering* (*ICTCE*), Singapore, 2020, pp. 35–46.

[2] G. C. Alexandropoulos, I. Vinieratou, M. Rebato, L. Rose, and M. Zorzi, Uplink beam management for millimeter wave cellular MIMO systems with hybrid beamforming, in *Proc. 2021 IEEE Wireless Communications and Networking Conf.* (*WCNC*), Nanjing, China, 2021, pp. 1–7.

[3] A. Singh and S. Joshi, A survey on hybrid beamforming in MmWave massive MIMO system, *J. Sci. Res.*, vol. 65, no. 1, pp. 201–213, 2021.

[4] J. Palacios, N. González-Prelcic, C. Mosquera, and T. Shimizu, A dynamic codebook design for analog beamforming in MIMO LEO satellite communications, in *Proc. 2022 IEEE Int. Conf. Communications* (*ICC*), Seoul, Republic of Korea, 2022, pp. 1–6.

[5] M. Mahmood, A. Koc, and T. Le-Ngoc, Massive-MIMO hybrid precoder design using few-bit DACs for 2D antenna array structures, in *Proc. 2021 IEEE Int. Conf. Communications* (*ICC*), virtual, 2021, pp. 1–5.

[6] E. Balti, Hybrid precoding for mmWave V2X doubly-selective multiuser MIMO systems, arXiv preprint arXiv: 2103.09444, 2021.

[7] X. Zhang and F. Zhao, Hybrid precoding algorithm for millimeter-wave massive MIMO systems with subconnection structures, *Wirel. Commun. Mob. Comput.*, vol. 2021, p. 5532939, 2021.

[8] A. J. Ortega, OMP-based hybrid precoding and SVD-based hybrid combiner design with partial CSI for massive MU-MIMO mmWave system, in *Proc. 2020 Int. Conf. Communications, Signal Processing, and their Applications* (*ICCSPA*), Sharjah, United Arab Emirates, 2021, pp. 1–5.

[9] H. Ayad, M. Y. Bendimerad, and F. T. Bendimerad, Hardware phase shift hybrid precoding designs for multi-user massive MIMO systems, *J. Phys.*: *Conf. Ser.*, vol. 2134, p. 012027, 2021.

[10] B. Al-Nahhas, M. Obeed, A. Chaaban, and M. J. Hossain, RIS-aided cell-free massive MIMO: Performance analysis and competitiveness, in *Proc. 2021 IEEE Int. Conf. Communications Workshops* (*ICC Workshops*), Montreal, Canada, 2021, pp. 1–6.

[11] I. Yildirim, A. Koc, E. Basar, and T. Le-Ngoc, RIS-aided angular-based hybrid beamforming design in mmWave massive MIMO systems, in *Proc. 2022 IEEE Global Communications Conf.* (*GLOBECOM*), Rio de Janeiro, Brazil, 2023, pp. 5267–5272.

[12] M. Cui, Z. Wu, Y. Chen, S. Xu, F. Yang, and L. Dai, Demo: low-power communications based on RIS and AI for 6G, in *Proc. 2022 IEEE Int. Conf. Communications Workshops* (*ICC Workshops*), Seoul, Republic of Korea, 2022, pp. 1–2.

[13] L. Hu, G. Li, X. Qian, D. W. Kwan Ng, and A. Hu, Joint transmit and reflective beamforming for RIS-assisted secret key generation, in *Proc. 2022 IEEE Global Communications Conf.* (*GLOBECOM*), Rio de Janeiro, Brazil, 2023, pp. 2352–2357.

[14] Q. Zhu, H. Li, R. Liu, M. Li, and Q. Liu, Hybrid beamforming and passive reflection design for RIS-assisted mmWave MIMO systems, in *Proc. 2021 IEEE Int. Conf. Communications Workshops* (*ICC Workshops*),

Montreal, Canada, 2021, pp. 1–6.

[15] K. Liu, Z. Zhang, and L. Dai, User-side RIS: Realizing large-scale array at user side, in *Proc. 2021 IEEE Global Communications Conference* (*GLOBECOM*), Madrid, Spain, 2022, pp. 01–06.

[16] R. Schroeder, J. He, and M. Juntti, Passive RIS *vs*. hybrid RIS: A comparative study on channel estimation, in *Proc. 2021 IEEE 93rd Vehicular Technology Conf.* (*VTC2021-Spring*), Helsinki, Finland, 2021, pp. 1–7.

[17] Y. Zhu, Z. Bo, M. Li, Y. Liu, Q. Liu, Z. Chang, and Y. Hu, Deep reinforcement learning based joint active and passive beamforming design for RIS-assisted MISO systems, in *Proc. 2022 IEEE Wireless Communications and Networking Conf.* (*WCNC*), Austin, TX, USA, 2022, pp. 477–482.

[18] N. T. Nguyen, Q. D. Vu, K. Lee, and M. Juntti, Spectral efficiency optimization for hybrid relay-reflecting intelligent surface, in *Proc. 2021 IEEE Int. Conf. Communications Workshops* (*ICC Workshops*), Montreal, Canada, 2021, pp. 1–6.

[19] N. T. Nguyen, Q. D. Vu, K. Lee, and M. Juntti, Hybrid relay-reflecting intelligent surface-assisted wireless communication, arXiv preprint arXiv: 2103.03900, 2021.

[20] N. T. Nguyen, J. He, V. D. Nguyen, H. Wymeersch, D. W. K. Ng, R. Schober, S. Chatzinotas, and M. Juntti, Hybrid relay-reflecting intelligent surface-aided wireless communications: Opportunities, challenges, and future perspectives, arXiv preprint arXiv: 2104.02039, 2021.

[21] Y. Lu, M. Hao, and R. MacKenzie, Reconfigurable intelligent surface based hybrid precoding for THz communications, *Intelligent and Converged Networks*, vol. 3, no. 1, pp. 103–118, 2022.

[22] H. Niu, Z. Chu, F. Zhou, C. Pan, D. W. K. Ng, and H. X. Nguyen, Double intelligent reflecting surface-assisted multi-user MIMO mmwave systems with hybrid precoding, *IEEE Trans. Veh. Technol.*, vol. 71, no. 2, pp. 1575–1587, 2022.

[23] C. Huang, Z. Yang, G. C. Alexandropoulos, K. Xiong, L. Wei, C. Yuen, Z. Zhang, and M. Debbah, Multi-hop RIS-empowered terahertz communications: A DRL-based hybrid beamforming design, *IEEE J. Sel. Areas Commun.*, vol. 39, no. 6, pp. 1663–1677, 2021.

[24] L. Dai and X. Wei, Distributed machine learning based downlink channel estimation for RIS assisted wireless communications, *IEEE Trans. Commun.*, vol. 70, no. 7, pp. 4900–4909, 2022.

[25] J. Ye, S. Guo, and M. -S. Alouini, Joint reflecting and precoding designs for SER minimization in reconfigurable intelligent surfaces assisted MIMO systems, *IEEE Trans. Wirel. Commun.*, vol. 19, no. 8, pp. 5561–5574, 2020.

[26] Z. Zhou, N. Ge, Z. Wang, and L. Hanzo, Joint transmit precoding and reconfigurable intelligent surface phase adjustment: A decomposition-aided channel estimation approach, *IEEE Trans. Commun.*, vol. 69, no. 2, pp. 1228–1243, 2021.

[27] Y. Wang, X. Chen, Y. Cai, and L. Hanzo, RIS-aided hybrid massive MIMO systems relying on adaptive-resolution ADCs: Robust beamforming design and resource allocation, *IEEE Trans. Veh. Technol.*, vol. 71, no. 3, pp. 3281–3286, 2022.

[28] Q. Hu, Y. Cai, K. Kang, G. Yu, J. Hoydis, and Y. C. Eldar, Two-timescale end-to-end learning for channel acquisition and hybrid precoding, *IEEE J. Sel. Areas Commun.*, vol. 40, no. 1, pp. 163–181, 2022.

[29] Q. Sun, H. Zhao, J. Wang, and W. Chen, Deep learning-based joint CSI feedback and hybrid precoding in FDD mmWave massive MIMO systems, *Entropy*, vol. 24, no. 4, pp. 441, 2022.

[30] X. Bao, W. Feng, J. Zheng, and J. Li, Deep CNN and equivalent channel based hybrid precoding for mmWave massive MIMO systems, *IEEE Access*, vol. 8, pp. 19327–19335, 2020.

[31] X. Li, Y. Huang, W. Heng, and J. Wu, Machine learning-inspired hybrid precoding for mmWave MU-MIMO systems with domestic switch network, *Sensors*, vol. 21, no. 9, pp. 3019, 2021.

[32] W. Ma, C. Qi, Z. Zhang, and J. Cheng, Sparse channel estimation and hybrid precoding using deep learning for millimeter wave massive MIMO, *IEEE Trans. Commun.*, vol. 68, no. 5, pp. 2838–2849, 2020.

[33] K. M. Attiah, F. Sohrabi, and W. Yu, Deep learning for channel sensing and hybrid precoding in TDD massive MIMO OFDM systems, *IEEE Trans. Wirel. Commun.*, vol. 21, no. 12, pp. 10839–10853, 2022.

[34] Q. Lu, T. Lin, and Y. Zhu, Channel estimation and hybrid precoding for millimeter wave communications: A deep learning-based approach, *IEEE Access*, vol. 9, pp. 120924–120939, 2021.

[35] I. S. Kim and J. Choi, Spatial wideband channel estimation for mmWave massive MIMO systems with hybrid architectures and low-resolution ADCs, *IEEE Trans. Wirel. Commun.*, vol. 20, no. 6, pp. 4016–4029, 2021.

[36] Y. Zhang, X. Dong, and Z. Zhang, Machine learning-based hybrid precoding with low-resolution analog phase shifters, *IEEE Commun. Lett.*, vol. 25, no. 1, pp. 186–190, 2021.

[37] X. Zhu, A. Koc, R. Morawski, and T. Le-Ngoc, A deep learning and geospatial data-based channel estimation technique for hybrid massive MIMO systems, *IEEE Access*, vol. 9, pp. 145115–145132, 2021.

[38] J. Shi, W. Wang, X. Yi, X. Gao, and G. Y. Li, Deep learning-based robust precoding for massive MIMO,

IEEE Trans. Commun., vol. 69, no. 11, pp. 7429–7443, 2021.

[39] Q. Wang, K. Feng, X. Li, and S. Jin, PrecoderNet: hybrid beamforming for millimeter wave systems with deep reinforcement learning, *IEEE Wirel. Commun. Lett.*, vol. 9, no. 10, pp. 1677–1681, 2020.

[40] K. Wei, J. Xu, W. Xu, N. Wang, and D. Chen, Distributed neural precoding for hybrid mmWave MIMO communications with limited feedback, *IEEE Commun. Lett.*, vol. 26, no. 7, pp. 1568–1572, 2022.

Girish Kumar N G received the BEng degree in electronics and communication engineering from Visvesvaraya Technological University, India, in 2005, the MS degree in intelligent systems from University of Sunderland, UK, in 2007, and the MEng degree from Visvesvaraya Technological University, India, in 2015. He is currently pursuing the PhD degree in electronics and communication engineering at Visvesvaraya Technological University, India. Currently, he is an assistant professor at the Department of Electronics and Telecommunication Engineering, Bangalore Institute of Technology, India. His research interests include massive MIMO communication, satellite communication, and error control coding. He is also a life time member of Indian Society for Technical Education (ISTE) and Institute of Engineers, India (IEI).

Sree Ranga Raju M N received the PhD degree in telecommunication engineering from Vinayaka Mission University, India, in 2011. He is currently a professor at Bangalore Institute of Technology, India. His research interests include mobile and wireless communications and networks, sensor networks, personnel communication services, high speed communication routing protocols, and wireless channel modelling. He has published 20+ international journal papers and headed as chairperson in several international and national conference. He was a panel member for reviewing research papers for several international conferences such as CICN 2010, 2011, 2012, ACT 2011, MIRA 2013, and WISE 2013.